Experimental Evaluation of the Punching Shear Strength of Interior Slab-column Connections with Different Shear Reinforcement Details

Rasha Mabrouk [1*], Gehad Younis [1], Osman Ramadan [1]

[1] *Structural Engineering Department, Faculty of Engineering, Cairo University, Cairo, Egypt.*

Abstract

This research aims to evaluate the effect of using different shear reinforcement details on the punching shear behavior of interior slab column connections. A comprehensive experimental program is conducted on sixteen specimens having the same concrete dimensions of $1100 \times 1100 \times 160$ mm where the slab depth is chosen to be less than that stipulated by different design codes. The parameters under examination were the type of shear reinforcement arranged in a cross shape perpendicular to the column edges (single leg, multi-leg, and closed stirrups), the spacing between stirrups (25 and 50 mm), and the extended length covered by the stirrups (300 and 425 mm). Experimental results showed that slabs reinforced with multi-leg or closed stirrups, even for slabs with a thickness of 160 mm, had an increase in the shear capacity by up to 40% depending on the stirrup amount. A noticeable enhancement in ductility was also observed. Slabs reinforced with vertical single-leg stirrups did not exhibit any improvements. A finite element analysis was conducted to further assess the punching shear behavior of the tested specimens. A comparison between the test results and values obtained using design codes such as ACI 318-19 and ECP 203-2018 showed that the two design codes give a rather underestimated prediction of the punching shear capacity.

Keywords: Punching Shear; Single-Leg Stirrups; Multi-Leg Stirrup; Closed Stirrup; Ductility; ANSYS.

1. Introduction

The flat plate system is one of the most widely used floor systems due to its many advantages, such as ease of reinforcement detailing, speedy construction, a reduction in the overall building height, and flexibility of changes in the architectural layout. However, the problem of punching shear stresses is one of the major disadvantages in the design of flat plates where brittle failure can occur at the slab-column connection due to the high punching stresses resulting from shear forces and unbalanced moments transferred between the column and the slab. Available research work that studied the punching shear of column-slab connections focused on many different parameters that affect their behavior, such as: the type and ratio of the shear reinforcement, distribution, and arrangement of reinforcement, concrete compressive strength, yield strength of reinforcement, and thickness of the slab [1]. Using shear reinforcement at the slab column connection was found to be an effective solution to avoid the brittle punching failure and to effectively improve the punching shear capacity. Many types of shear reinforcement are available and are reported in the literature, such as studs, shear heads, and open or closed stirrups.

This research focuses on the use of both open-leg and closed stirrups. The ACI 318-19 [2] allows different types of stirrups, such as single-leg, multi-leg, and closed stirrups. The Egyptian code of practice, ECP 203-2018 [3], allows using closed stirrups only. While the European code, Euro Code 2 [4], considers stirrups that enclose both the

---

top and bottom flexural reinforcement of the slab. Although installation of stirrups may be time-consuming, stirrups are cheap, easy to fix, and allow the reinforcement arrangements to pass through the column. These advantages make stirrups potentially a straightforward and cost-effective method compared to other types of punching shear reinforcement.

Various past research has been conducted on the effect of shear reinforcement on the behavior of flat slabs. Papanikolaou et al. [5] tested a total of 30 slabs with and without shear reinforcement. Shear reinforcement consisted of either bent-up bars or closed stirrups. They concluded that ACI 318-19 [2] is conservative in predicting the shear strength of stirrups while the Eurocode is less conservative, leading to unsafe design at high shear reinforcement ratio. The same results were reported by Lips et al. [1]. They tested sixteen full-scale slab specimens with and without shear reinforcement. The shear reinforcement types used were studs and stirrups. They concluded that the effect of size and slab slenderness ratio is irrelevant to the presence of shear reinforcement if failure occurs due to crushing of the concrete strut. In their experimental results, Hegger et al. [6] tested 39 interior slab-column connections. They concluded that punching shear reinforcement with well anchoring significantly increases the shear capacity and ductility of a flat slab-column connection. Mabrouk et al. [7] tested seven half-scale specimens to show the contribution of horizontal flexural reinforcement and vertical shear reinforcement in the form of closed stirrups on the punching behavior of reinforced concrete flat slabs. They concluded that adding vertical stirrups was effective in enhancing the punching shear capacity. Broms [8] tested three specimens and compared them to two reference specimens with shear studs tested previously to study the behavior of cages with inclined stirrups on flat slabs.

Issa et al. [9] tested twelve interior slab-column connections to investigate the effect of using a new improved distribution technique of closed stirrups with variable width on the punching shear strength. They concluded that by using the new distribution of shear reinforcement, the strength of the slab-column connections was increased. Schmidt et al. [10] tested eleven interior slab-column connections with a variable shear reinforcement ratio. They concluded that the load-increase is less pronounced for larger ratios and seems to result in an upper limit. Raafat et al. [11] tested eight interior slab-column connections with variable slab thickness, stirrup yielding stress, stirrup shape (closed and multi-leg), and extended length to investigate their effect on shear strength. They concluded that when stirrups were extended to a distance from the column edge that was more than twice the slab thickness, the punching capacity increased by 8.2%.

Polak et al. [12] recommended using stirrups to enhance both strength and ductility for slabs greater than 250 mm having poor anchorage details, while for thinner slabs, special attention to the anchorage details should be taken into consideration. Broms [13] found that using a combination of stirrups and bent-up bars gave excellent results in improving the ductility of flat plates. He again tested the same system [14] and found that using a combination of stirrups and bent-up bars over a specific large area around the column is very effective in creating an extremely ductile structural system. Eom et al. [15] tested eight slab specimens reinforced with continuous hoops. They found that the maximum punching strength occurred early for specimens having a low shear reinforcement ratio, while for slabs having a high shear reinforcement ratio, the maximum strength occurred at large deflection and the shear reinforcement reached its yield strain in this case. Beutel and Hegger [16] showed that the anchorage behavior of links could be upgraded if transverse welded bars were placed. Yang et al. [17] used stirrups and ring beams to reinforce their specimens. They found that there is good enhancement in post-punching performance of junction when reversing loading direction. De Oliveira et al. [18] tested nine interior slab-column connections with variable anchorage detailing of closed stirrups. They concluded that the punching shear resistance and the behavior of the slabs were not affected by the change in anchorage conditions.

Considering the vertical stirrup type shear reinforcement, tests have indicated that shear reinforcement improves punching capacity of flat slabs even for slabs with small thickness. However, good anchorage is needed in this case. Design codes, on the contrary, put limitations on the minimum thickness required to use shear reinforcement. On the other hand, shear reinforcement details are usually different among the approaches used by the different design codes. For example, the Egyptian design code ECP 203-2018 [3] permits only the use of closed stirrups as shear reinforcement for resisting punching shear stresses, while the American Code ACI 318-19 [2] allows different types of stirrups, such as single-leg, multi-leg, or closed stirrups. Few studies were provided for well-anchored open leg stirrups with multiple numbers of legs.

Spacing between stirrups is an important factor that affects the capacity and behavior of the slab column connection. Studies have dealt with that parameter, however smaller values for spacing were rarely used in previous research. Smaller stirrup spacing results in a higher steel area that can resist stresses at the critical punching section. Additionally, close spacing between stirrups helps minimizing cracks in the critical area [7]. The length of extension of the stirrups beyond the column face was not seen much in previous research. Investigation is needed to assess its effect and limitations on the punching behaviour.

1.1. Research Significance

This research aims at studying the behavior of flat slabs using different types of stirrups. The thickness of the specimens used was taken as 160 mm which is lower than the limit set by both ECP 203-2018 [3] and ACI 318-19 [2] to determine the effectiveness of using stirrups in this case. The parameters under study are: 1) The shape of stirrups in the form of single leg stirrups, multi leg stirrups with 2, 4 and 6 branches, and closed stirrups with 2 and 4 branches, 2) The spacing between the stirrups where relatively small values of 25 and 50 mm were used, and 3) The extended length of the shear reinforcement from the face of the column. The ratio of the shear reinforcement is considered through the value of the spacing between the stirrups and the number of branches within the critical shear perimeter. Also, the width of the stirrups was changed with the detailing of the different types used. Sixteen specimens were divided into four groups of reinforced concrete flat plates each having a certain type of shear reinforcement to investigate the reliability of the different types of shear reinforcement in resisting the punching shear stresses. The behavior of the slab column connections was evaluated through the cracking patterns, modes of failure, load deflection, and load strain curves. Following that, a finite element analysis using ANSYS as well as a comparison with different design codes were conducted to study the suitability of these provisions in the evaluation of the punching shear capacity. A flow chart of the research methodology is shown in Figure1.
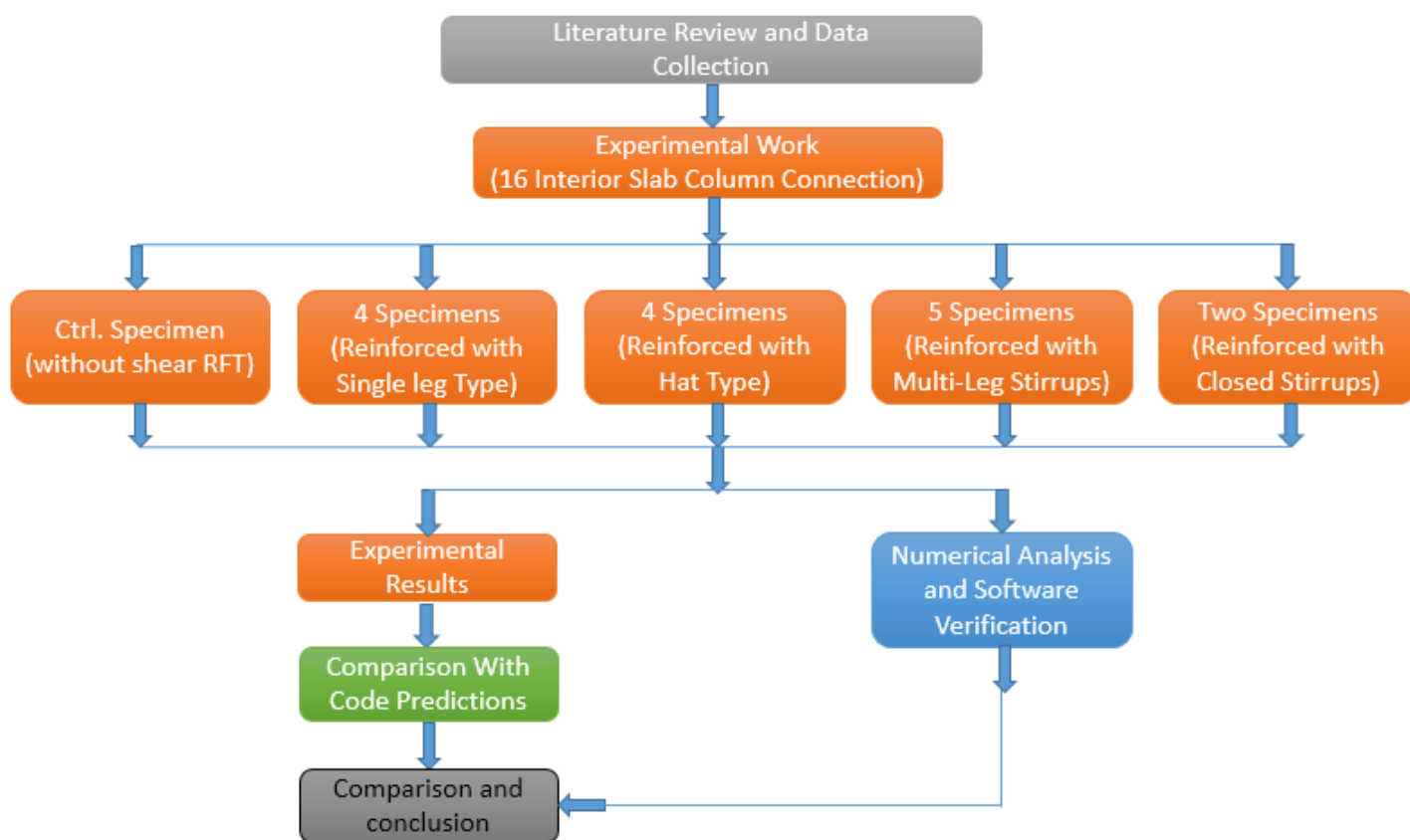

Figure 1. Research methodology flow chart

## 2. Experimental Program

2.1. Specimen Details

Sixteen interior slab-column connections were cast and tested at the Concrete Research Laboratory at Cairo University. Details of the specimens are summarized in Table 1. All tested slab specimens had the same concrete dimensions of $1100 \times 1100 \times 160$ mm thickness with a central stub column of dimensions 150×150 mm and 200 mm height. The effective depth was 140 mm with a concrete cover of 20 mm. The specimens had the same longitudinal reinforcement meshes where a flexural reinforcement ratio of 1.54% was selected for the tension reinforcement. This value was designed to prevent flexural failures for all tested slabs. A reinforcement ratio of 0.33% was used for the compression side reinforcement.

Table 1. Details of the tested specimens

Groups	Specimen	Shear Reinforcement Details					
		S (mm)	L (mm)	B (mm)	N	Ratio (%)	Type
Control	**S1**	-	-	-	-		-
I	S2-I	50	300 (2.3d)	-	1	0.36	Single-Leg stirrups
	S3-I	25	300 (2.3d)	-	1	0.72	
	S4-I	50	425 (3.3d)	-	1	0.36	
	S5-I	25	425 (3.3d)	-	1	0.72	
II	S6-II	50	300 (2.3d)	200 (1.5d)	2	0.72	Multi-Leg open stirrups
	S7-II	25	300 (2.3d)	200 (1.5d)	2	1.44	
	S8-II	50	425 (3.3d)	200 (1.5d)	2	0.72	
	S9-II	25	425 (3.3d)	200 (1.5d)	2	1.44	
III	S10-III	50	300 (2.3d)	520 (4d)	4	0.72	
	S11-III	25	300 (2.3d)	520 (4d)	4	1.44	
	S12-III	50	425 (3.3d)	520 (4d)	4	0.72	
	S13-III	25	425 (3.3d)	520 (4d)	4	1.44	
	S14-III	50	425 (3.3d)	750 (6d)	6	1.44	
IV	S15-IV	50	425 (3.3d)	200 (1.5d)	2	0.72	Closed stirrups
	S16-IV	50	425 (3.3d)	520 (4d)	4	0.72	

* Notes: S is spacing between stirrups; L is stirrups extended length; B is stirrups width; N is number of stirrup branches.

One control specimen was cast with no shear reinforcement to be used as a reference while the other fifteen specimens had different types of stirrups. The details of all stirrup types are shown in Figure 2. The fifteen specimens with shear reinforcement were divided into four groups. Within each group two parameters were studied; first the extended length of the stirrups measured from the face of the column till the last stirrup used and here referred to as L and second, the spacing between stirrups referred to as S. Figure 3 presents the concrete dimensions and boundary conditions for all slabs and the typical longitudinal reinforcement details. Figure 4 introduces the typical shear reinforcement details for each group.
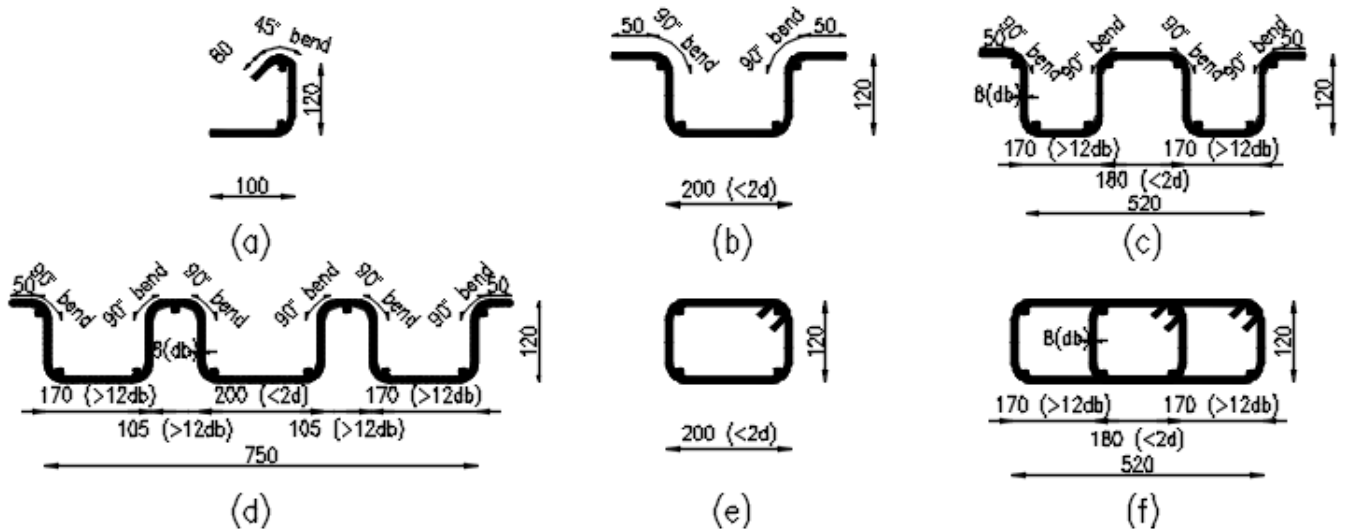
Figure 2. Details of different types of stirrups (measured in mm): a) Single-leg, b) 2-branches (Hat type), c) 4-branches multi-leg, d) 6-branches multi-leg, e) 2-branches closed stirrups, f) 4-branches closed stirrups
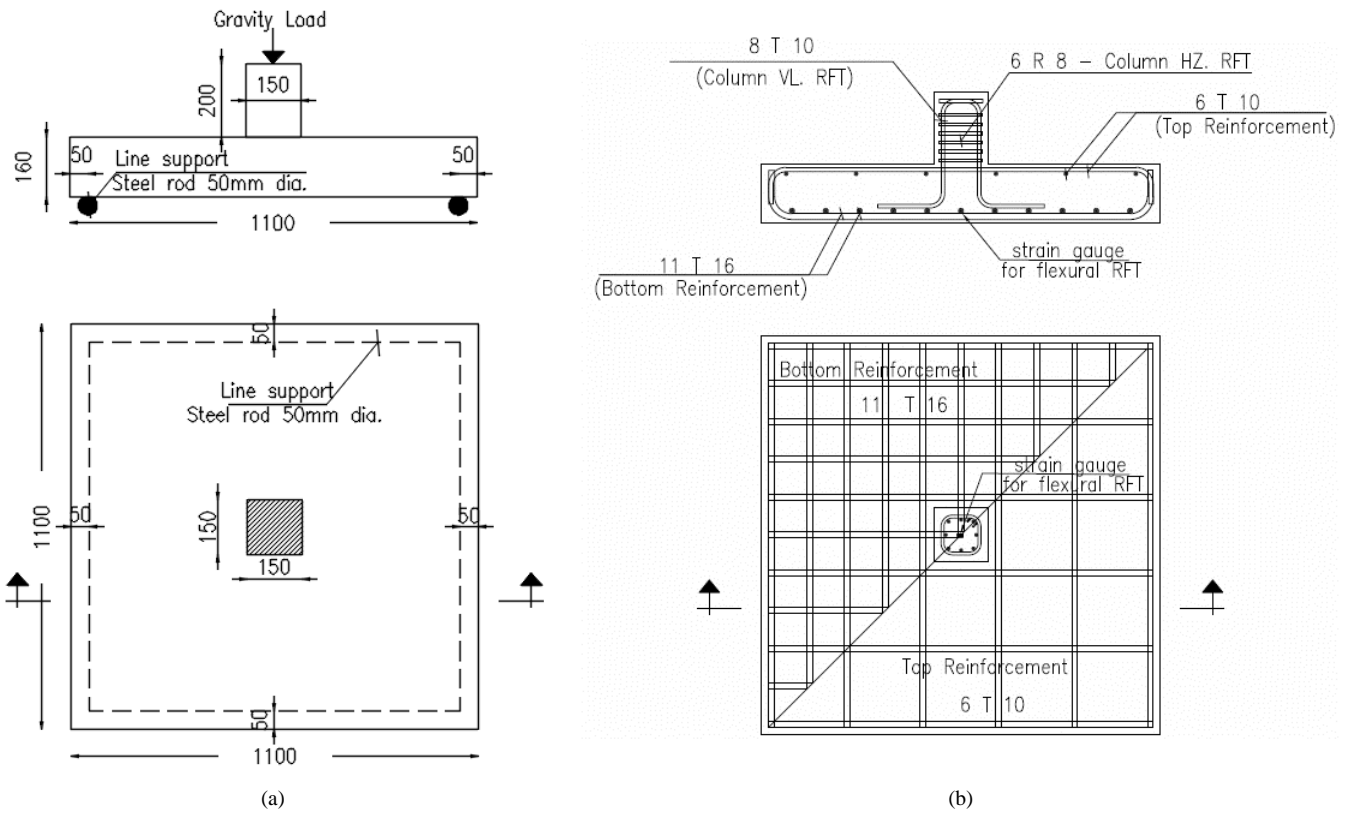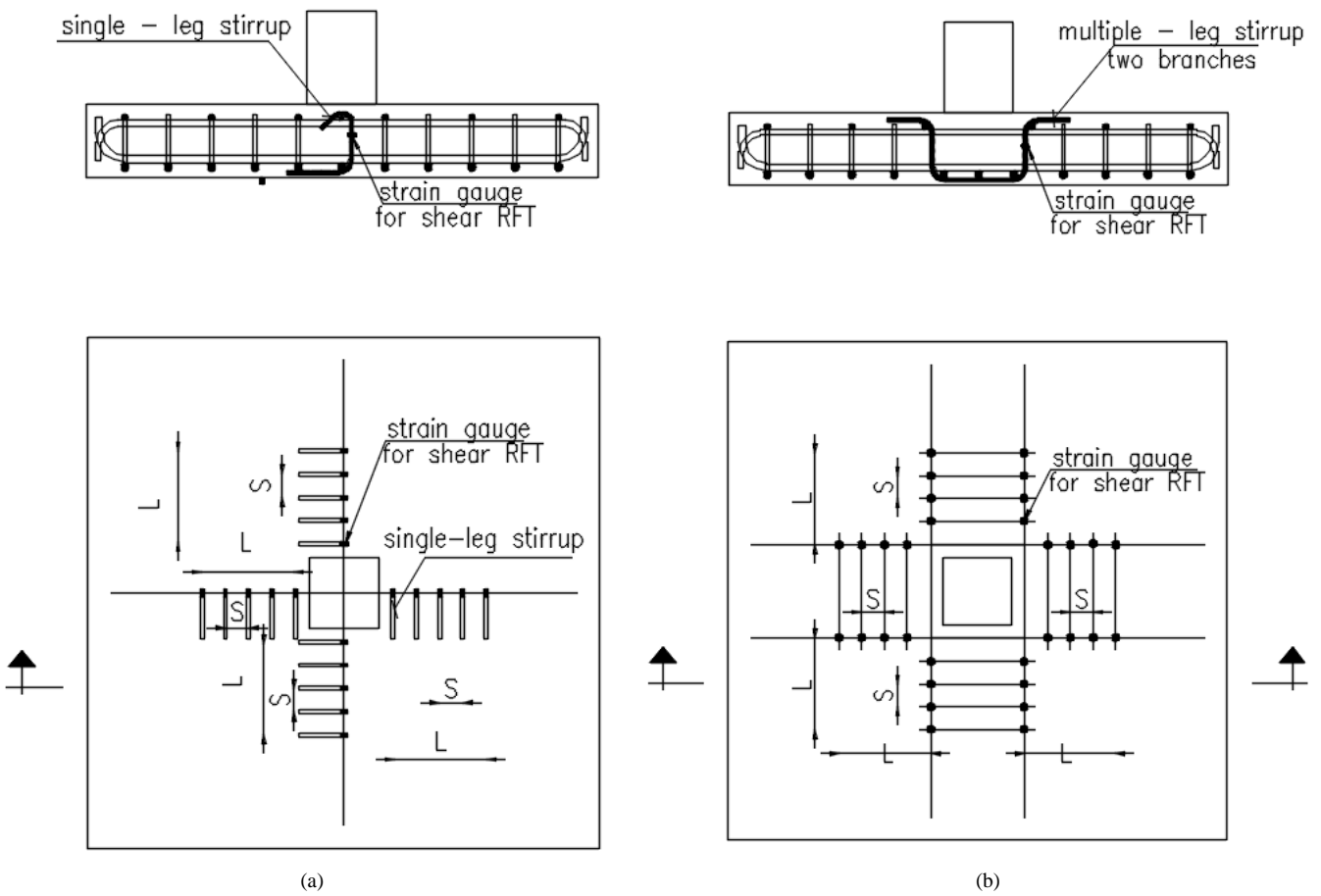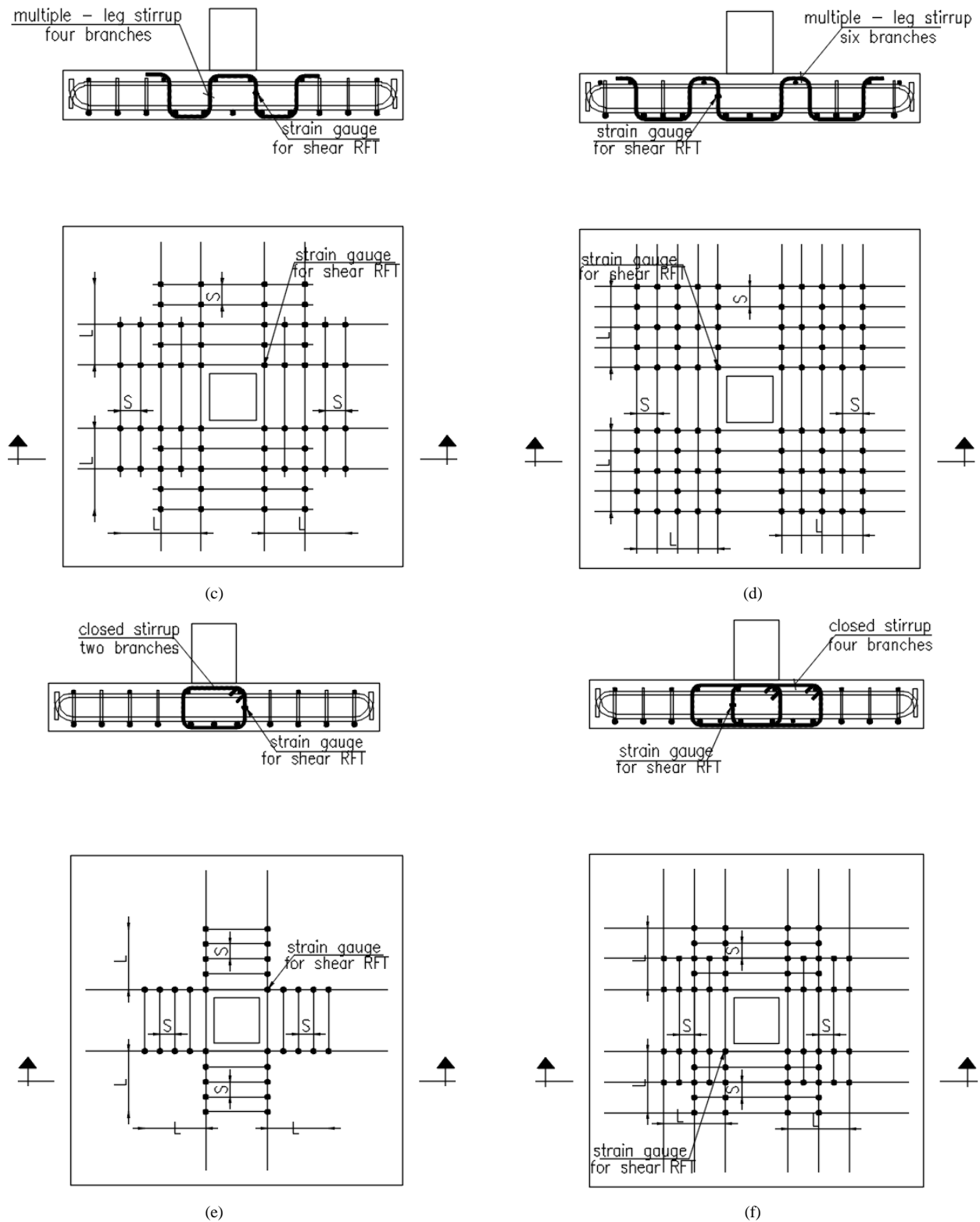
(a)

(b)

Figure 3. Tested specimen: a) Boundary condition and geometry, b) Typical main reinforcement and location of strain gauges

(a)

(b)

Figure 4. Typical shear reinforcement details and location of stirrup's strain gauge for: a) group I, b) group II, c) group III, except (S14-III), d) S14-III, e) Group IV (S15-IV), f) Group IV (S16-IV)

Group I contained four specimens that represented single leg stirrups type. Groups II and III contained specimens having multi leg stirrups type of two, four, and six branches, respectively. Group IV contained two specimens that represented closed stirrups type of two and four branches aiming to study the effect of this type on the punching shear strength. These shear reinforcement detailing were chosen as they represent the types that are easily applicable in the Egyptian market where this study tried to cover all the possible variations of single and multi-leg stirrups. The spacing between stirrups, S, were taken as 25 and 50 mm. These two values represent 0.18d and 0.36d, respectively. The maximum allowable value for the spacing, S, is 0.5d as per the provisions of ACI 318-19 [2] and ECP 203-2018 [3]. The commonly used value in practice and previous research was 0.5d. In this research, the authors experiment with the smaller values of 0.18d and 0.36d which is expected to show a noticeable effect on the punching behaviour.

The width of the stirrups, B, was changed between the different groups as the type of stirrups changed where it varied between 1.5d and 4d and for only one specimen S14-III it was taken 6d. Stirrup width was increased as the number of branches increased to maintain that the flexural reinforcement is enclosed by the vertical stirrups. The middle two branches were kept at a distance less than 2d for all groups while the distances between the other branches were kept greater than 12 d_b, where d_b is the stirrup diameter as per ACI 318-19 [2] provisions. The number of branches was varied through the same group (III) to increase the shear reinforcement ratio as seen in Table 1 and Figure 2. The shear reinforcement ratio was calculated at the critical perimeter lying at 0.5d from the face of the column and its value changed between 0.36% and 1.44% thus covering a wide range of values to show the behavior on the low and high end of reinforcement ratios.

The inner critical shear perimeter is reported to lie at 0.5d from the face of the column while the outer critical section lies at 2d [2, 3]. Two values were selected for the extended length of stirrups, L, such that the stirrups lie within the outer critical shear perimeter in one case and extend beyond it in the other. Thus, L was taken as 300 mm representing 2.1d and 425 mm representing 3d where it extends till the end of the specimen in this case.

2.2. Material Properties

The concrete mix design for all specimens was prepared based on a target 28-day cubic strength of 30 MPa. Ordinary Portland cement type I 52.5N, crushed limestone of maximum aggregate size of 10 mm, natural sand, clean water, and admixtures were used in the mix. The results of sieve analysis for fine and coarse aggregates are shown in Figure 5. The compressive strength of the concrete was determined using compressive strength conducted on samples cast with the specimens using cubic forms of 150 mm side length. The average measured cubic compressive strength at testing day was 33.5 MPa. A commercial steel reinforcement from a local company that complies with Egyptian standards ESS was used. Reinforcement of grades 360 were used for steel bars with 10 mm and 16 mm diameters and reinforcement of grade 240 was used for the stirrups. These are the common reinforcement grades available in the Egyptian market. The nominal yield strain of 1800 and 1200 $\mu\varepsilon$ were assumed for both grades 360 and 240 respectively.
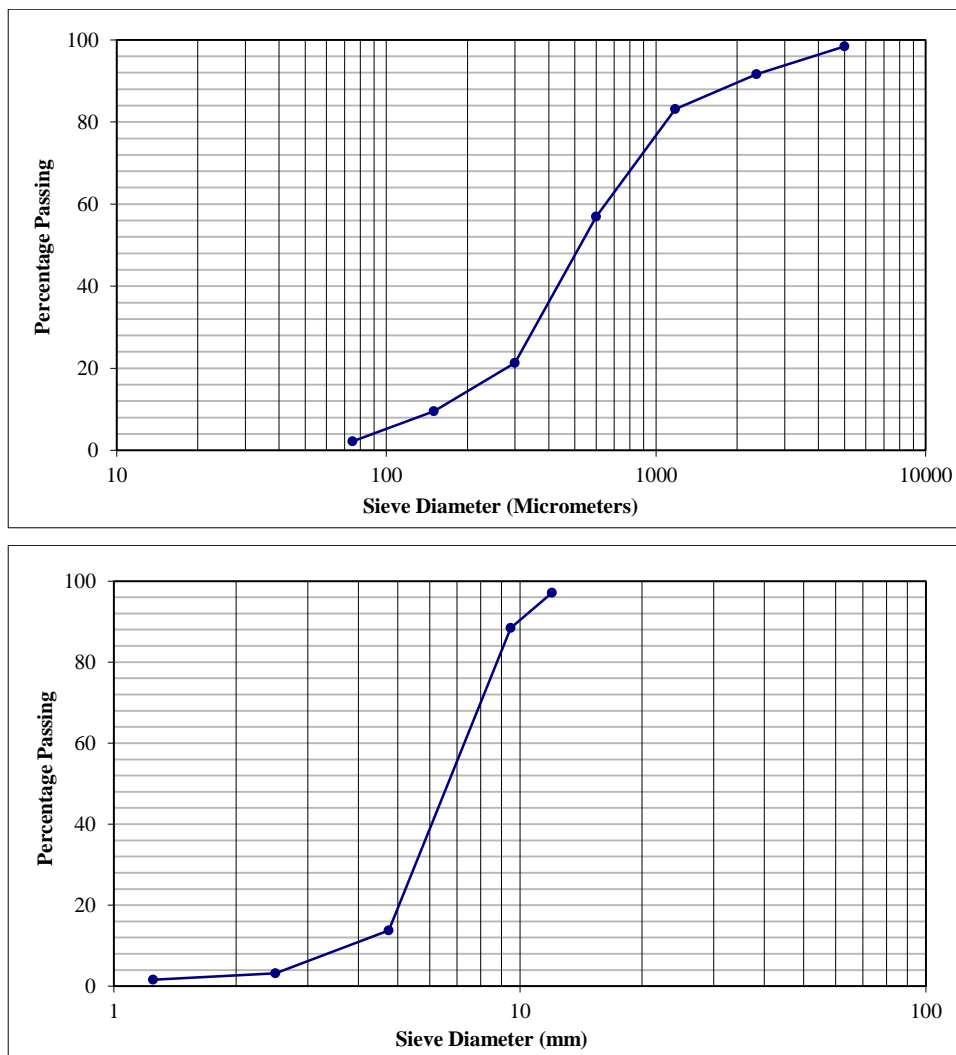
Figure 5. Sieve analysis results for: a) Fine Aggregate, b) Coarse Aggregate

2.3. Test Setup and Instrumentation

The specimens were loaded upside down on a steel space truss connected and rested on the laboratory floor as shown in Figure 6 with the clear span of the specimens taken as 1000 mm. A concentric load was introduced using a hydraulic jack applied to the stub column at the center of the specimens. Loads were recorded using a load cell and deflections at the bottom of slab were recorded using three linear variable displacement transducers (LVDTs) located at middle span and quarter spans. Strain in the reinforcement bars was measured using strain gauges of 10 mm length with their locations shown in Figures 1 and 2.
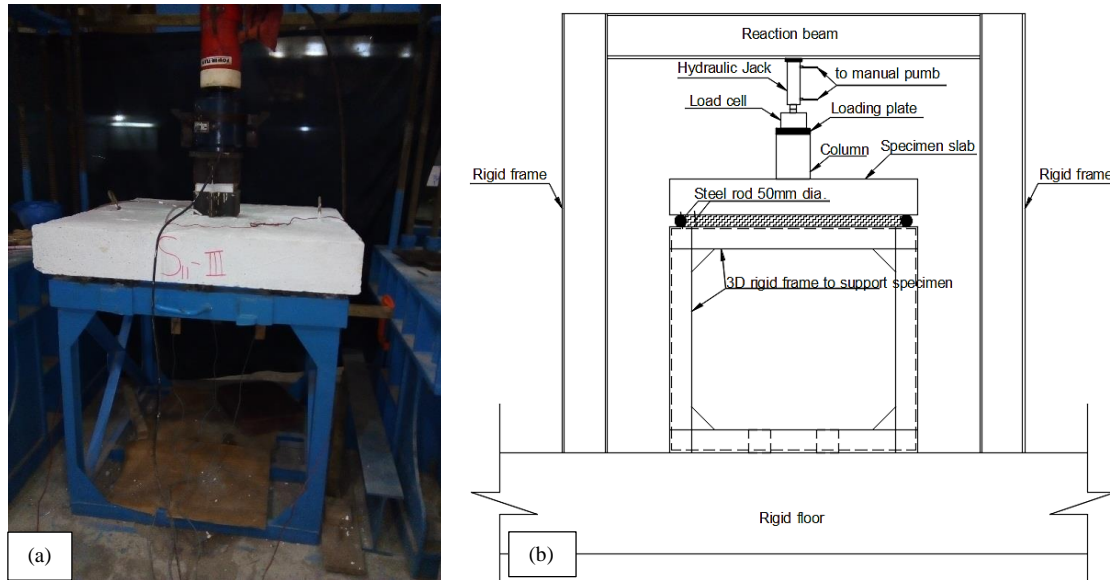
Figure 6. Test setup: a) photo, b) schematic drawing

3. Experimental Results and Discussion

Experimental results were analyzed such as first crack, cracking patterns, load-deflection curves, and load-strain curves to provide the physical meaning and knowledge about the behavior of each specimen. Test results for all specimens are shown in Table 2. Visual inspection was done in each slab specimen to determine the first crack and the cracking patterns up to failure. First crack load and peak load with its corresponding deflection and strain in both flexural and shear reinforcement are given and gathered through the software used in laboratory. Only the stirrup's strain readings of specimen S9-II were not recorded because of an experimental error during concrete compacting using the vibrator.

Table 2. Specimen test results

Specimen ID	First Crack load (kN)	V_u (kN)	V_{flex} (kN)	V_u/V_{flex}	Δ_u (mm)	ε_f (µm/m)	ε_s (µm/m)	Mode of failure
S1	200	515	838	0.61	13.07	2133	-	Punching
S2-I	220	498	849	0.59	9.29	2117	129	Punching
S3-I	220	533	845	0.63	12.02	2274	97	Punching
S4-I	160	532.5	845	0.63	11.54	1844	423	Punching
S5-I	230	524	845	0.62	11.13	2257	255	Punching
S6-II	200	668	864	0.77	10.10	2857	727	Punching
S7-II	200	681.5	864	0.79	12.54	2917	1152	Punching
S8-II	210	640.5	849	0.75	12.40	2657	625	Punching
S9-II	180	688	849	0.81	14.05	1899	NA	Punching
S10-III	200	627	864	0.73	9.52	3590	1253	Punching
S11-III	210	620	867	0.72	14.86	2412	1346	Flexural-Punching
S12-III	200	606.5	867	0.70	12.50	1707	1561	Flexural-Punching
S13-III	200	682.5	867	0.79	13.51	1754	1217	Flexural-Punching
S14-III	180	736	838	0.88	18.29	3417	1366	Flexural-Punching
S15-IV	220	600	864	0.69	10.08	2349	418	Punching
S16-IV	200	706.5	838	0.84	22.00	3043	2040	Flexural-Punching

V_u: Ultimate test load, V_{flex}: calculated flexural capacity of specimen; Δ_u: Mid span deflection at ultimate load (mm); ε_f: Flexural reinforcement strain at ultimate load (µm/m); ε_s: Stirrup strain at ultimate load (µm/m).

The flexural capacity was calculated using the yield line theory, as shown in Figure 7. According to Ghali et al. [19], the load producing flexural failure can be obtained using equation (1). The calculated flexural capacity, V_{flex}, exceeded the punching capacity for all slabs which assures punching failure.

$$V_{flex} = \frac{8ml_s}{l_1 - c} \tag{1}$$

where m is the moment per unit slab width at yielding of the bottom flexural reinforcement, l_s is the dimension of the slab specimen, l_1 is the span between the supports.
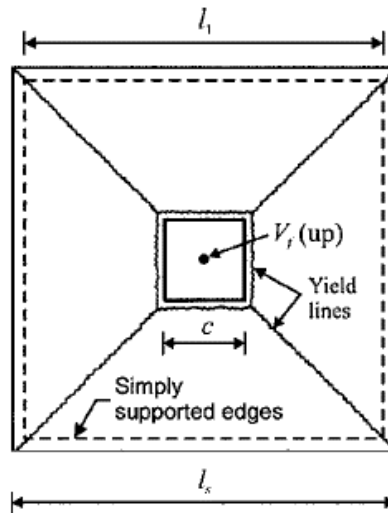
Figure 7. Fracture yield pattern: isotropic square slab specimen with square column subjected to axial force V_{flex} on column (Ghali et al. [19]

3.1. Cracking Patterns and Modes of Failure

The values of the first crack load of all specimens are close to each other except for specimens S4-I, S9-II, and S14-III. This is as predicted since the capacity of the slabs up to the cracking point is controlled only by the concrete strength. The decrease in the cracking load for specimens S4-I, S9-II, and S14-III can be due to weak bonding between concrete and flexural steel and may be due to some of the honeycomb at the intersection between the column with slab.

Figure 8 to Figure 13 show the typical crack patterns at failure load for the tension side for the different groups. The actual patterns for all tested specimens are shown in Figure 14 to Figure 19. In general, all samples showed a similar crack pattern before reaching the peak load. As the specimens were loaded, radial cracks started to form at the center column and advance towards the edge of the specimen. As the loading increased, transverse cracks started to develop radially and extend forming larger circumferences. Only specimen S1, without shear reinforcement, failed in a sudden brittle mode with loud sound. The mode of failure of groups I, II, and S15-IV specimens was a brittle punching failure mode. Whereas group III and S16-IV specimens failed in a mixed flexural-punching mode. Although saw-cuts were not performed, an inclination of failure crack can be approximately determined. Column height was recorded before and after loading and the column penetration for all specimens ranged between 5 mm and 20 mm.
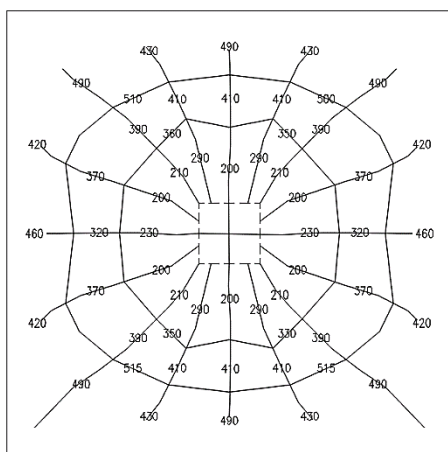

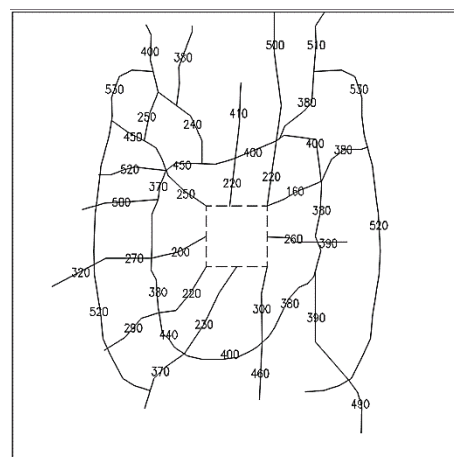**Figure 8. Schematic drawing of crack pattern for control specimen S1**

Figure 9. Typical drawing of crack pattern for Group I
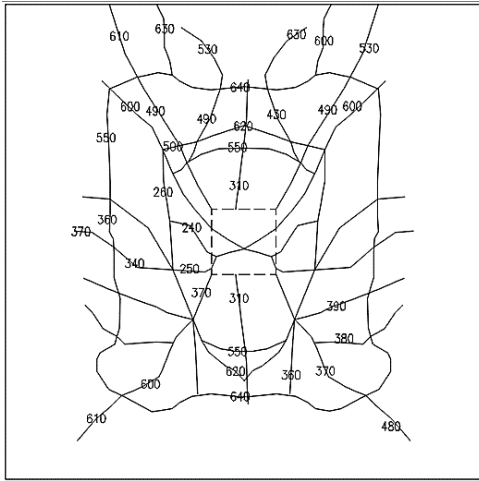
Figure 10. Typical drawing of crack pattern for Group II
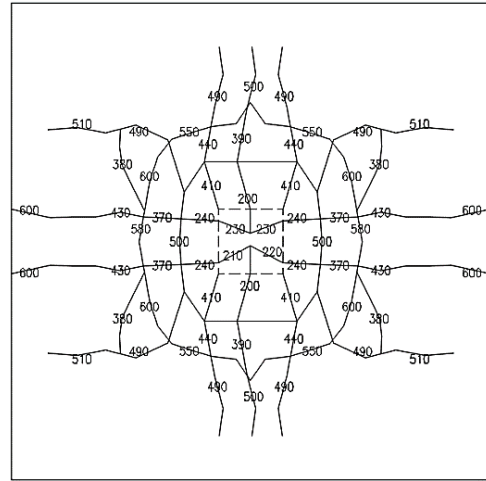

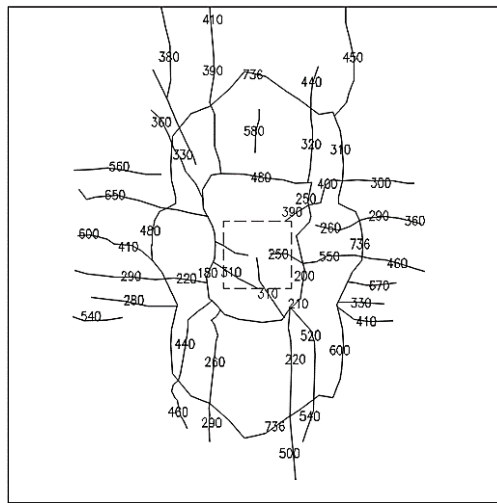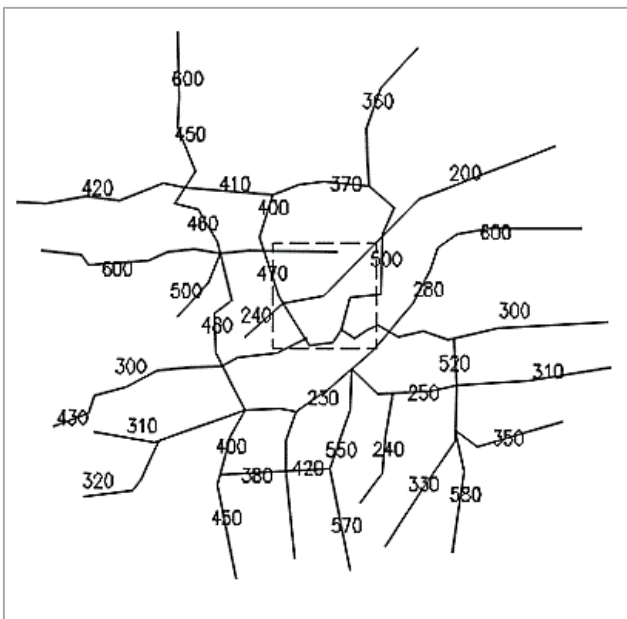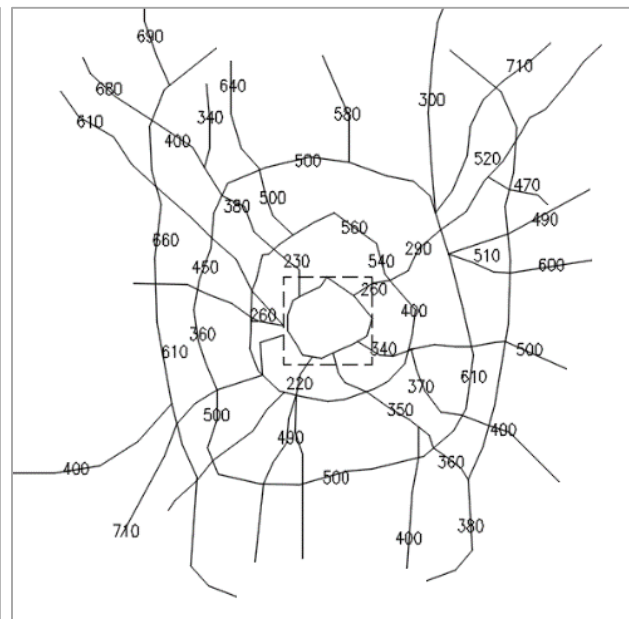**Figure 11. Typical drawing of crack pattern for Group III**

Figure 12. Schematic drawing of crack pattern for specimen S14-III

(a)

(b)

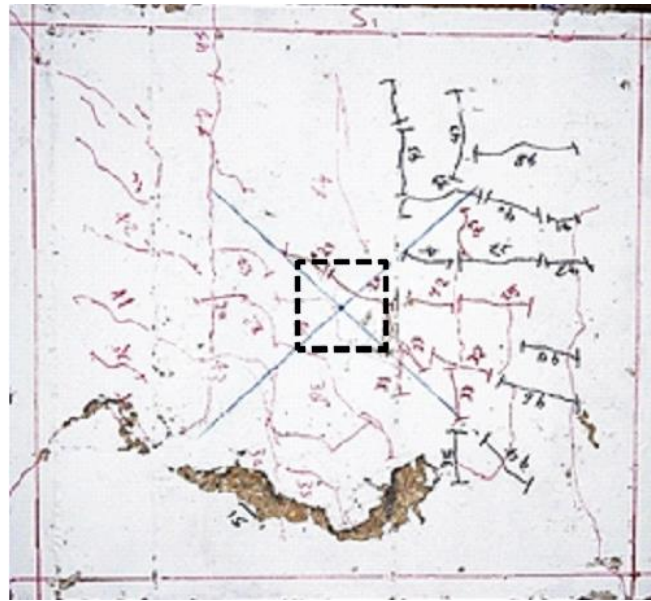**Figure 13. Typical drawing of crack pattern for specimens: a) S15-IV, and b) S16-IV**

Figure 14. Crack pattern of control specimen S1
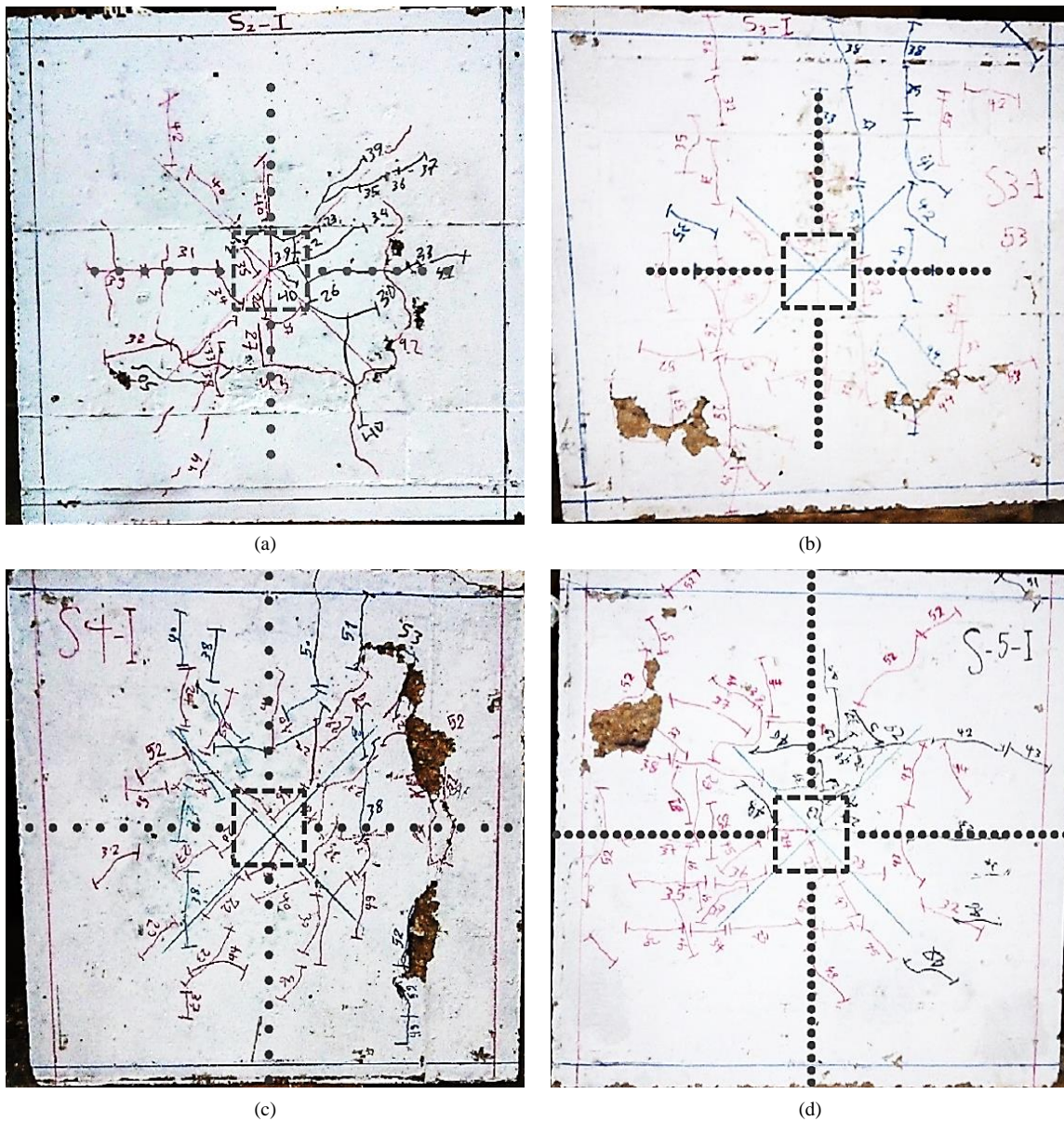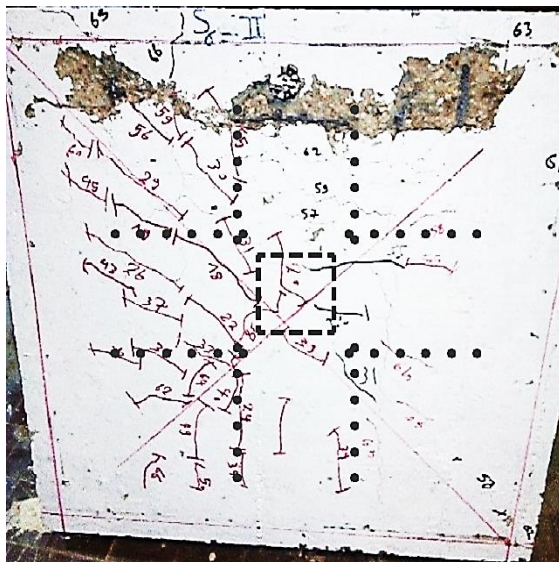

(a)	(b)
(c)	(d)

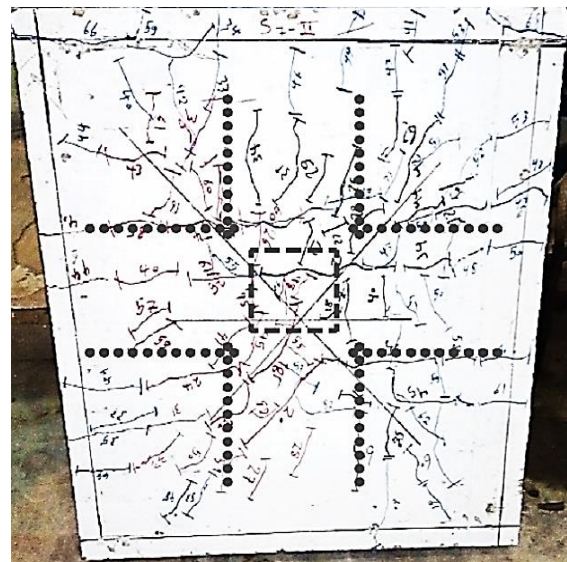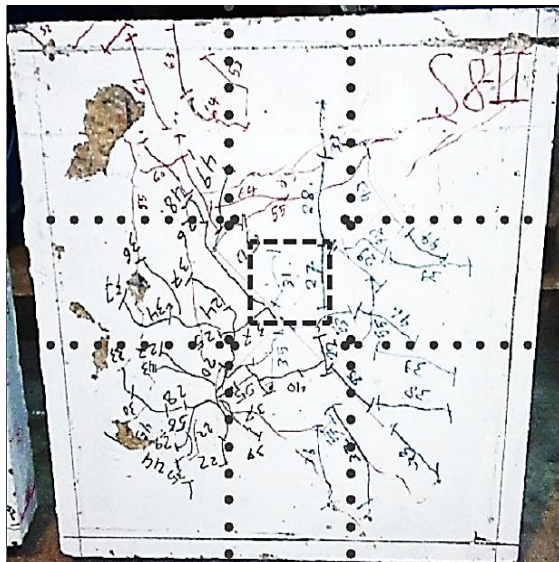**Figure 15. Crack pattern of specimens in Group I: a) S2-I, b) S3-I, c) S4-I, and d) S5-I**
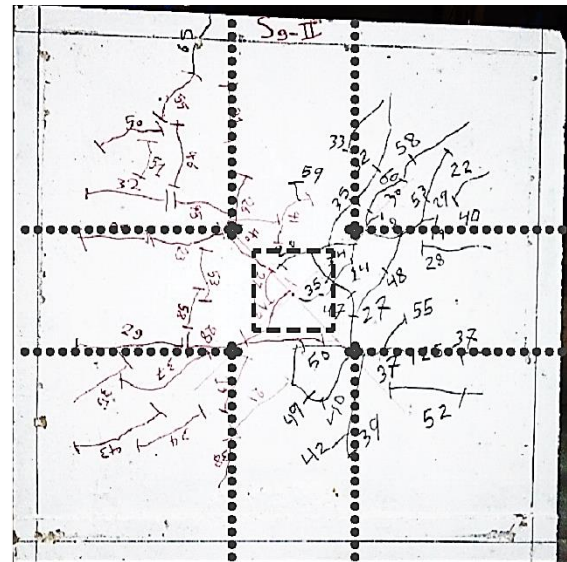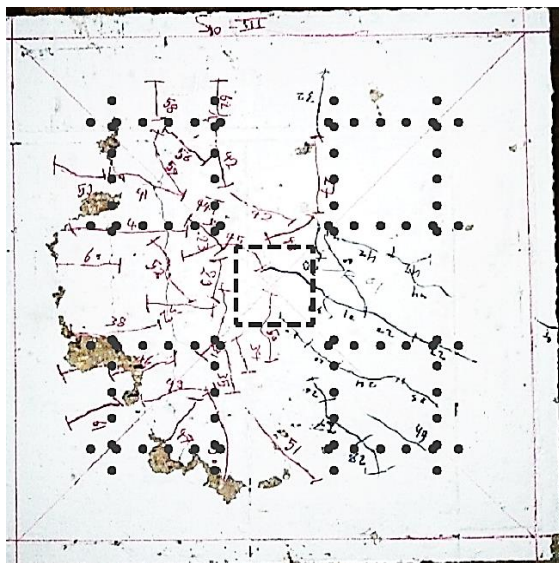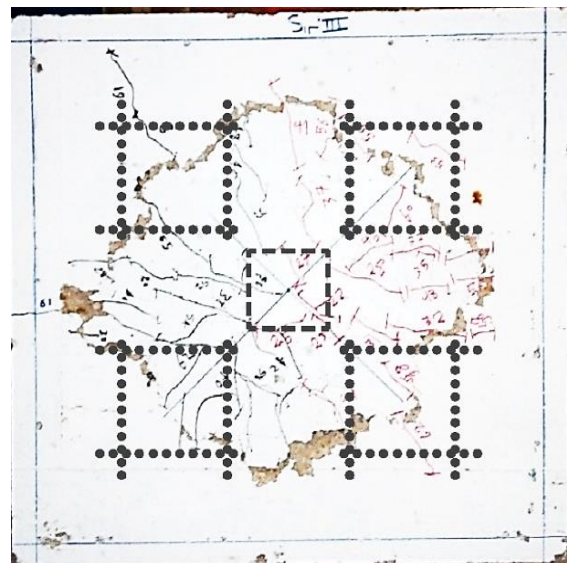
Figure 16. Crack pattern of specimens in Group II: (a) S6-II, (b) S7-II, (c) S8-II, and (d) S9-II
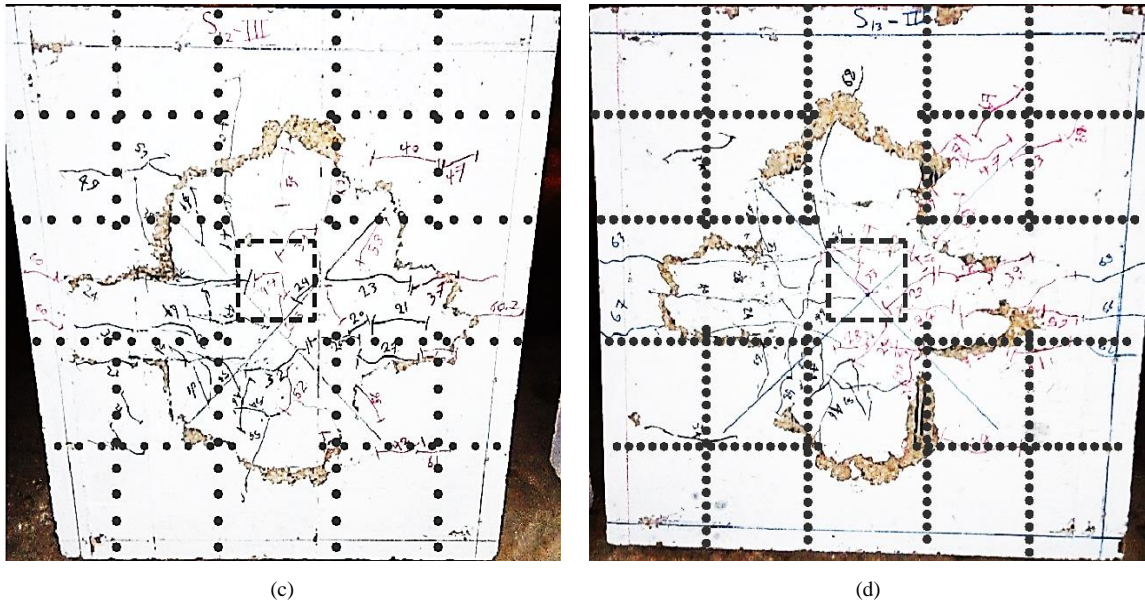
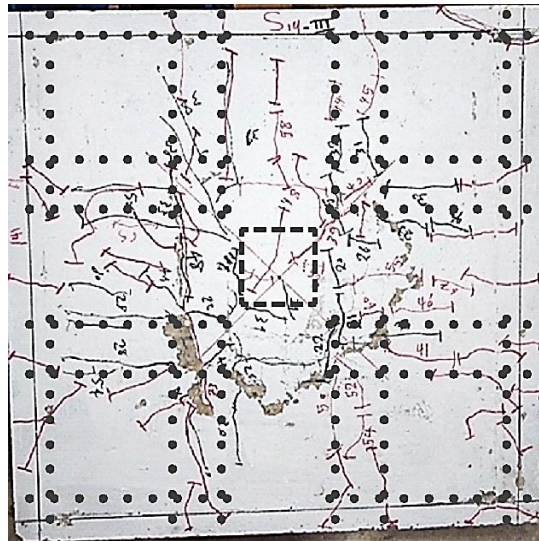**Figure 17. Crack pattern of specimens in group III: a) S10-III, b) S11-III, c) S12-III, and d) S13-III**

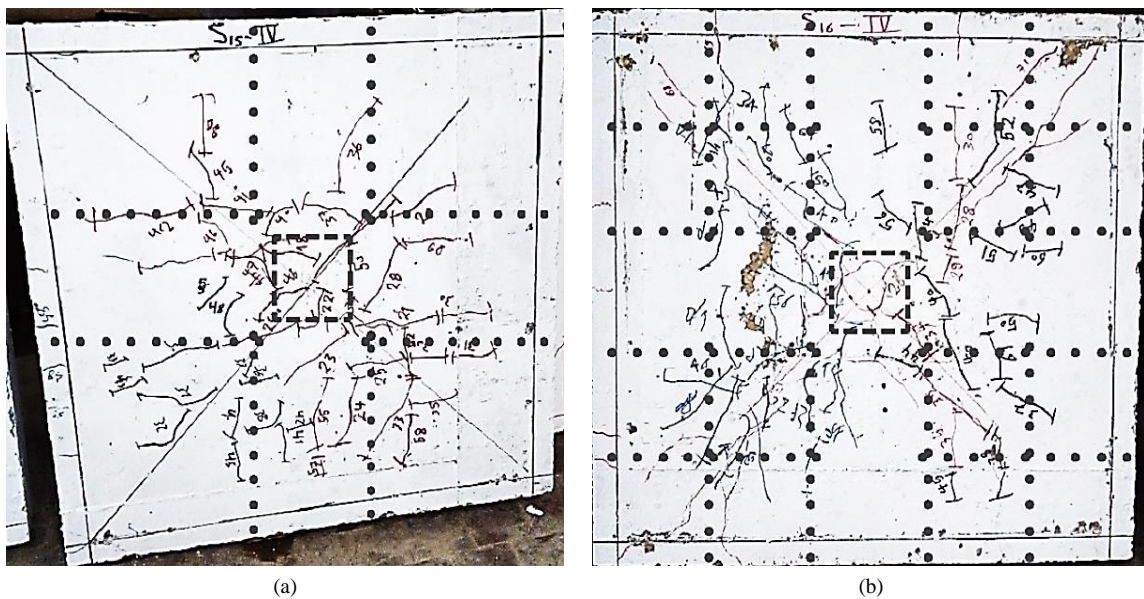**Figure 18. Crack pattern of specimen S14-III**

Figure 19. Crack pattern of specimens in group IV: (a) S15-IV, and (b) S16-IV

Figures 9 and 10 shows the schematic crack pattern of groups I and II respectively. The failure surface seems to be inside the shear reinforced zone for specimens S2-I, S4-I, S5-I, and S8-II (Also see Figures 15 and 16). When decreasing the spacing from 50 mm to 25 mm (100% decrease), a relatively flat inclined failure crack formed. Figures 11, 12, and 13-b show the schematic crack pattern of group III and specimen S16-IV respectively. The failure surface occurred inside the shear reinforced zone for all specimens except S10-III (Also see Figures 17, 18, and 19 (b)). For group I and II specimens, failure crack formation seems to be more steeply inclined compared to S1.

Figure 13 shows the schematic crack pattern of specimens S15-IV and S16-IV. For specimen S15-IV, a steeper inclined failure crack was formed compared to all other specimens. The failure surface happened around the column zone indicating failure by crushing of the concrete strut close to the column. (As also seen in Figure 19 -a). Whereas specimen S16-IV failed in almost flexural failure mode where failure surface formed inside the shear reinforced zone accompanied with exceeding the yield strength of the flexural reinforcement.

3.2. Load-Deflection Behavior

Figure 20 shows the load deflection curves for each of the four groups compared to the control specimen. All specimens reinforced with shear reinforcement recorded higher stiffness compared to the control specimens. Except for specimen S2-I, all specimens reinforced with shear reinforcement showed different degrees of improvement in both the punching shear strength and ductility of the slabs. Specimen S14-III having multi-leg stirrup with 6 branches recorded the maximum load and reached a punching strength increase of 43% compared to specimen S1. The ductility and post punching behavior are significantly affected by the type of shear reinforcement. Peak load sudden drop was observed for the control specimen (S1), Group I specimens, Group II specimens S6-II and S7-II, and S15-IV (closed stirrups with two branches). This shows that stirrups with lower number of branches did not show any post punching behavior accompanied with less ductility compared to other specimens.
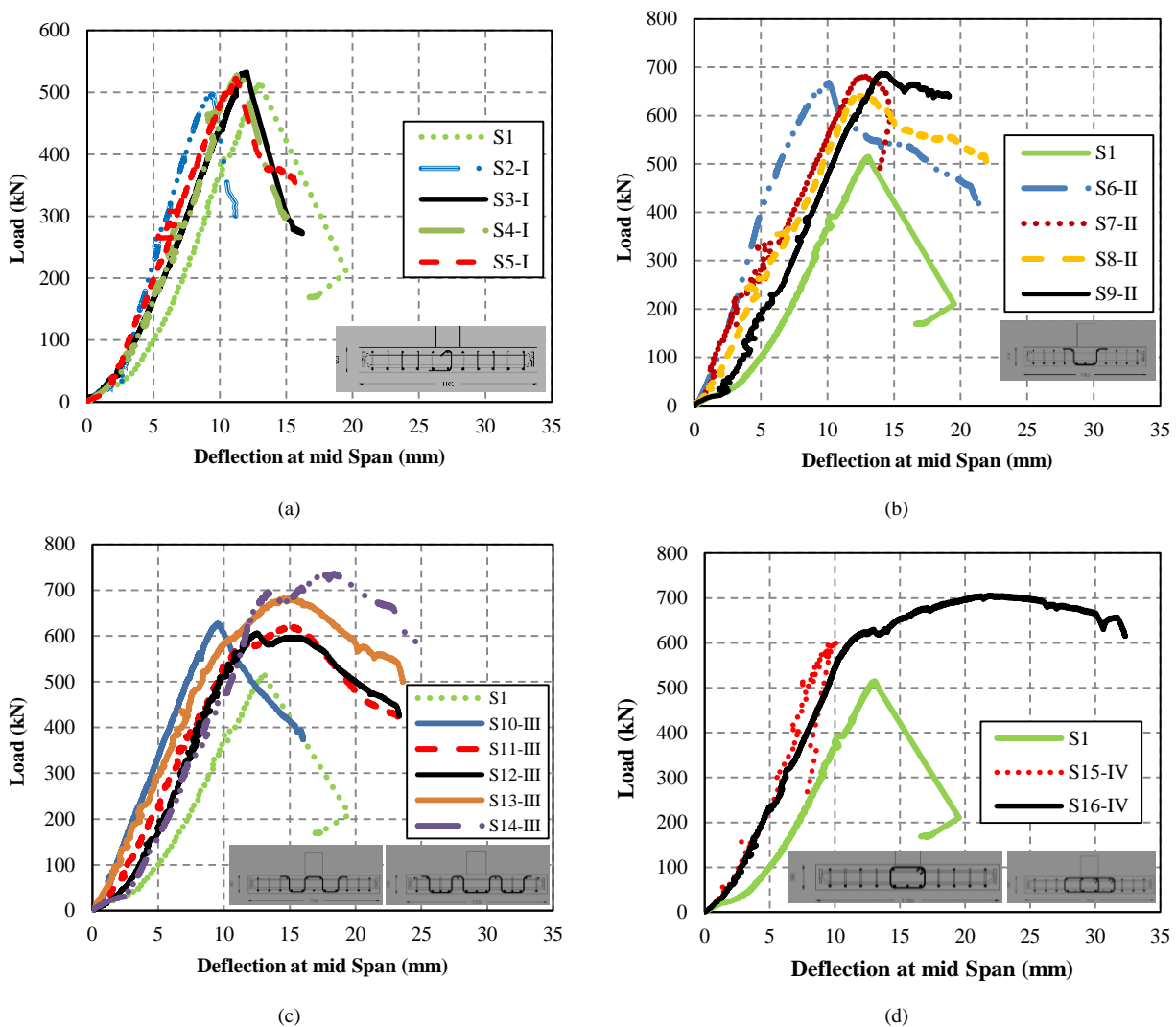

(a)

(b)

(c)

(d)

Figure 20. Load deflection curves for the four groups: (a) Group I, (b) Group II, (c) Group III, and (d) Group IV

Figure 20-a shows the influence of single-leg stirrups, reinforced with different spacing and extended length, on the punching shear strength. Specimens S2-I, S3-I, S4-I, and S5-I reached a punching strength value of about 97%, 103.5%, 103%, and 102% of the control specimen S1, respectively. Specimen S2-I recorded slight decrease in failure load compared to control one which could be due to some errors during specimen preparation in the laboratory. Not much increase in shear strength or ultimate deflection for the specimens in Group I was observed which is due to the large spacing between vertical legs in the tangential direction. When decreasing the spacing from 50 mm to 25 mm which led to an increase in the reinforcement ratio from 0.36% to 0.72%, specimen S3-I recorded a slight increase in punching strength by about 7% compared to specimen S2-I whereas no strength gaining was recorded when comparing specimen S4-I to S5-I. On the other hand, when increasing the extended length from 300 mm (≈2.3d) to 425 mm (≈3.3d), specimen S4-I recorded a slight increase in punching strength by about 7% compared to specimen S2-I whereas no strength gaining was recorded when comparing specimen S3-I to S5-I.

Figure 20-b represents the influence of multi-leg stirrups having two branches, reinforced with different spacing and extended length shown in group II. In comparison to the control specimen S1, specimens S6-II, S7-II, S8-II, and S9-II reached a punching strength about 130%, 132%, 124%, and 134% from the capacity of S1, respectively. Shear strength increased compared to group I because of the good distribution of stirrup legs through the two branches where group I had only one leg of stirrups. Group II specimens failed in a punching mode. No significant increase in punching capacity was recorded when the spacing was decreased for the value of extended length of 300 mm. However, for the longer extended length of 425 mm an increase in punching strength was reached by about 7% when comparing specimen S8-II to S9-II. Also, no significant increase in capacity was observed when the extended length was increased for the lower shear reinforcement ratio of 0.72% while a slight increase can be seen at the specimens with reinforcement ratio of 1.44%. In fact, specimen S8-II showed a slightly lower punching capacity than S6-II. This is due to the change in failure mode where the punching failure occurred outside the reinforcement zone for specimen S6-II and inside the zone for specimen S8-II.

The results of the specimens in group III are shown in Figure 20-c where the influence of multi-leg stirrups having 4 and 6 branches can be seen. In comparison to the control specimen S1, specimens S10-III, S11-III, S12-III, and S13-III having four branches reached a punching strength about 122%, 120%, 118%, and 133%, respectively. The same pattern was observed for the punching capacity of these four specimens as for Group II except that the increase in punching capacity was more pronounced when the extended length was increased to 425 mm for the high reinforcement ratio of 1.44% where specimen S13-III showed an increase of 10% compared to slab S11-II. It should be noted that the punching shear strength of specimens reinforced with four branches is slightly less than those reinforced with two branches. Firstly, the specimens with four branches are defined as having the same reinforcement ratio as those with two branches because the critical shear perimeter for the two cases lies at 0.5d from the face of the column thus including only the first two branches which is supported by the cracking pattern in Figure 17. Thus, it is expected to have similar punching capacities for the two groups. However, the difference in capacities can be due to the change in the mode of failure where ductile failure inside shear reinforced zone occurred for specimens reinforced with four branches and brittle failure outside shear reinforced zone was observed for those reinforced with two branches. Finally, for specimen S14-III, having six branches, an increase of 43% in the ultimate load compared to S1 was observed.

Figure 20-d illustrates the influence of closed stirrups reinforced with 2 and 4 branches, reinforced with the same spacing and extended length, on the punching shear strength. In comparison to the control specimen S1, the capacity of specimens S15-IV and S16-IV increased by about 17%, and 37% respectively.

Figure 21 summarizes the cracking loads and ultimate loads for all the tested slabs. Using single leg stirrups does not have any advantages on the behavior of the slabs. In fact, the slabs in this case behave similar to the control specimen without shear reinforcement. Using multi leg stirrups and closed stirrups led to better results. Increasing the reinforcement ratio through the decrease in the spacing from 50 mm to 25 mm led to an increase in the capacity for specimens having multi leg stirrups. Increasing the shear reinforcement through having more branches for open leg stirrups within the critical shear zone leads to a more significant increase in the punching shear capacity as seen in specimen S14-III and S13-III compared to S12-III.

The effect of the type of shear reinforcement on the punching shear strength is shown in Figure 22 where the specimens were divided according to the reinforcement ratio and the extended length. For the same reinforcement ratio and extended length, stirrups having different shapes showed variable punching capacities. At 0.72% shear reinforcement ratio and extended length, L, of 300 mm, 2 branches open leg stirrups recorded the highest punching load. At 0.72% shear reinforcement ratio and extended length, L, of 425 mm, 4 branches closed stirrups recorded the highest punching load. At 1.44% shear reinforcement ratio and extended length, L, of 300 mm, 2 branches open leg stirrups recorded the highest punching load. At 1.44% shear reinforcement ratio and extended length, L, of 425 mm, 6 branches open leg stirrups recorded the highest punching load.
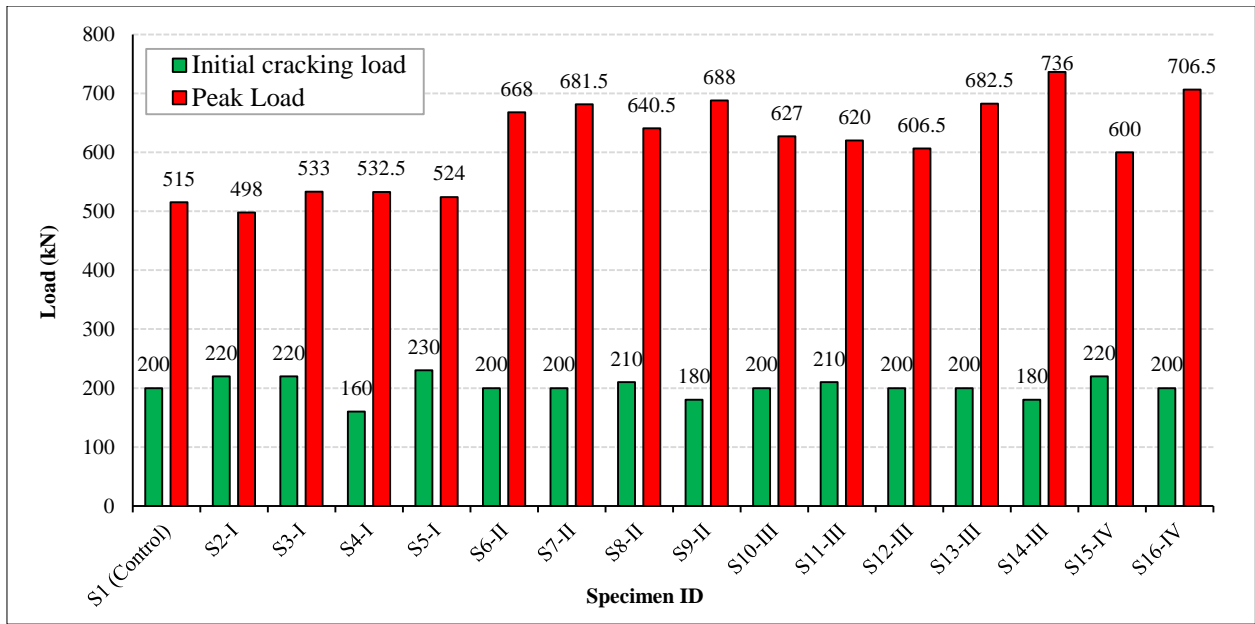
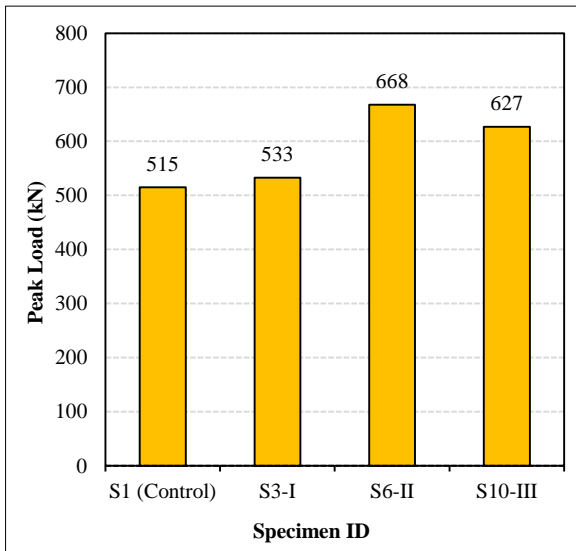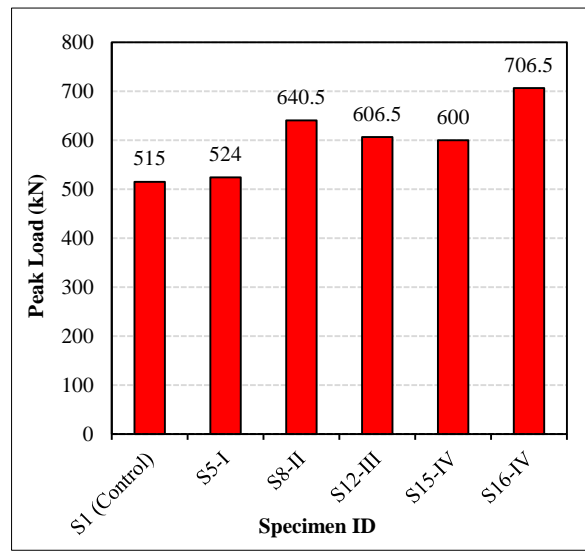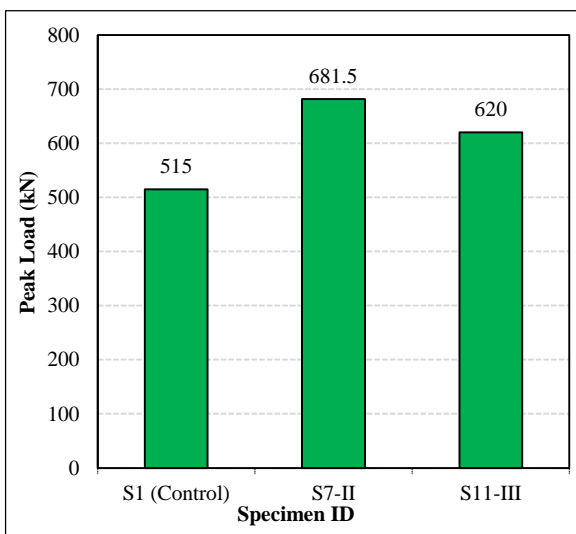**Figure 21. Cracking and peak load for all specimens**

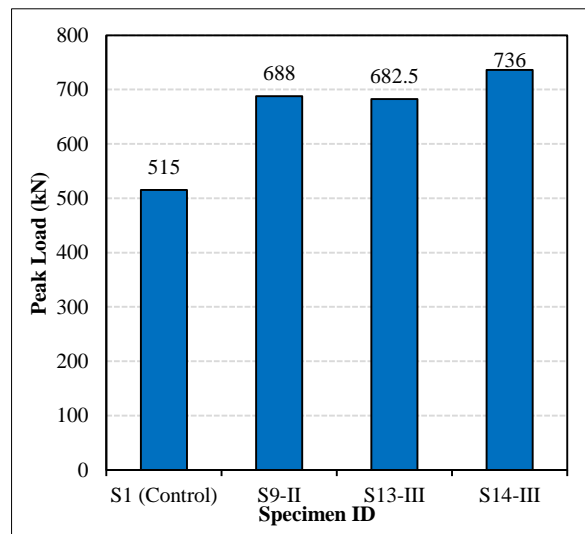**Figure 22. Effect of the type of shear reinforcement on peak load: a) 0.72% & L=300 mm, b) 0.72% & L=425 mm, c) 1.44% & L=300 mm, and d) 1.44% & L=425 mm**

For specimens having 4 branches, when comparing specimen S16-IV having closed stirrups to specimen S12-III having multi-leg stirrups, specimen S16-IV recorded an increase in punching strength by about 17% compared to specimen S12-III despite having the same reinforcement ratio. This can be explained due to the better confinement provided by the closed stirrups. However, for specimens having 2 branches and when choosing closed stirrups instead of multi-leg stirrups, no enhancement in shear capacity was found when comparing specimen S15-IV to specimen S8-II. This is due to the change in the mode of failure of S15-IV where failure due to crushing of the compression strut was observed as mentioned before. This premature failure may be due to the better anchoring of stirrups in specimen S15-IV compared to specimen S8-II resulting in very steep failure surface and the concrete strut seemed to be extensively crushed near the column face. A similar observation has also been made by Einpaul et al. [20]. The results also showed that increasing the stirrup width generally changes the failure pattern from brittle to ductile mode in addition to decreasing the perimeter of failure surface located inside the shear reinforced zone.

3.3. Load-Strain Behavior

Figure 23 represents the load strain curves of the flexural reinforcement measured at the column support for all specimens. The yield strain which is calculated as 1800 micro strain for the type of reinforcement used was reached at failure load for all specimens. However, the strain gauge in this case was located at the middle bar which means that this bar reached yield but not necessarily all bars have yielded. The mode of failure for each specimen was determined according to the shape and distribution of the cracking patterns and behavior of specimens. For specimen S16-IV, having closed stirrups of 4 branches, strain hardening was achieved. Therefore, it can be concluded that the closed stirrups having a width equals to column width plus twice slab depth significantly enhances the ductility of the slab-column connection compared to other types.
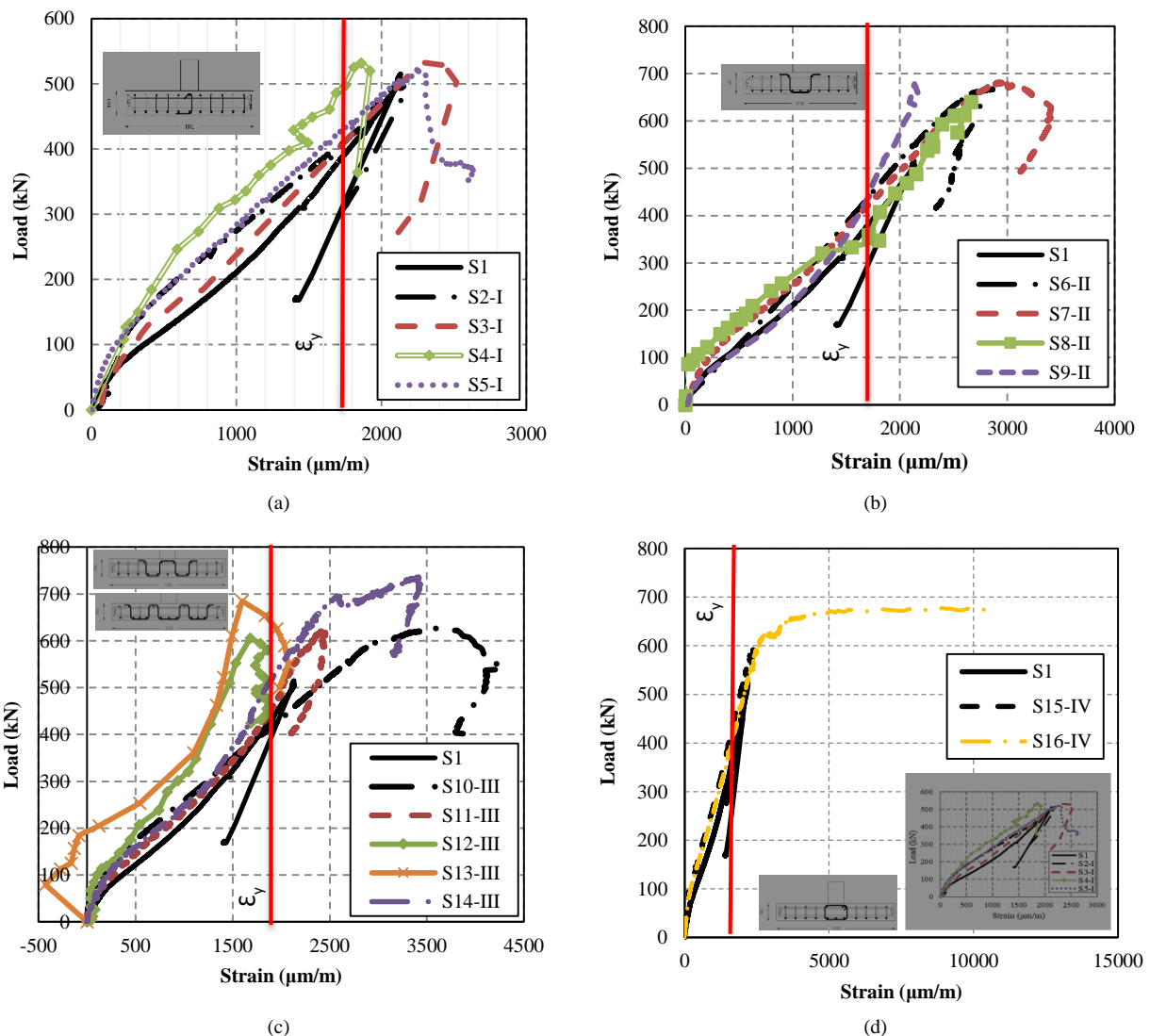

(a)

(b)

(c)

(d)

Figure 23. Load strain curves for the flexural steel for the four groups: a) Group I, b) Group II, c) Group III, and d) Group IV

Figure 24 shows the load strain relationship for the stirrups in all specimens except specimen S9-II where an error in the reading occurred due to damage of the strain gauge attached to the stirrup legs. The strain gauges were mounted on the stirrup branch located at 50 mm from the column face. Figure 24-a illustrates the strain in group I specimens reinforced with single leg type. The stirrups did not reach their yield strain which is calculated as 1200 micro strain and a brittle failure occurred. Figure 24-b shows the strain in group II specimens reinforced with two branch stirrups. It can be noted that only stirrup of specimen S7-II was yielded while other stirrup specimens did not reach the yield strain. Figure 24-c illustrates the strain in group III specimens, having 4 branches multi-leg stirrups. The strain measurements indicate that the stirrups reached the yield strain prior to reaching the peak load. As mentioned before this could be one of the reasons for the punching shear strength reduction when increasing the number of multi-leg stirrups from two branches to four branches which is that the failure mode was changed from brittle to ductile in addition to the fact that there was no bracing for the mid-flexural bar at the tension side. Figure 24-d shows the strain in group IV specimens reinforced with closed stirrups type. It can be noted that only stirrup of specimen S16-IV was yielded giving a mixed flexural- punching failure.
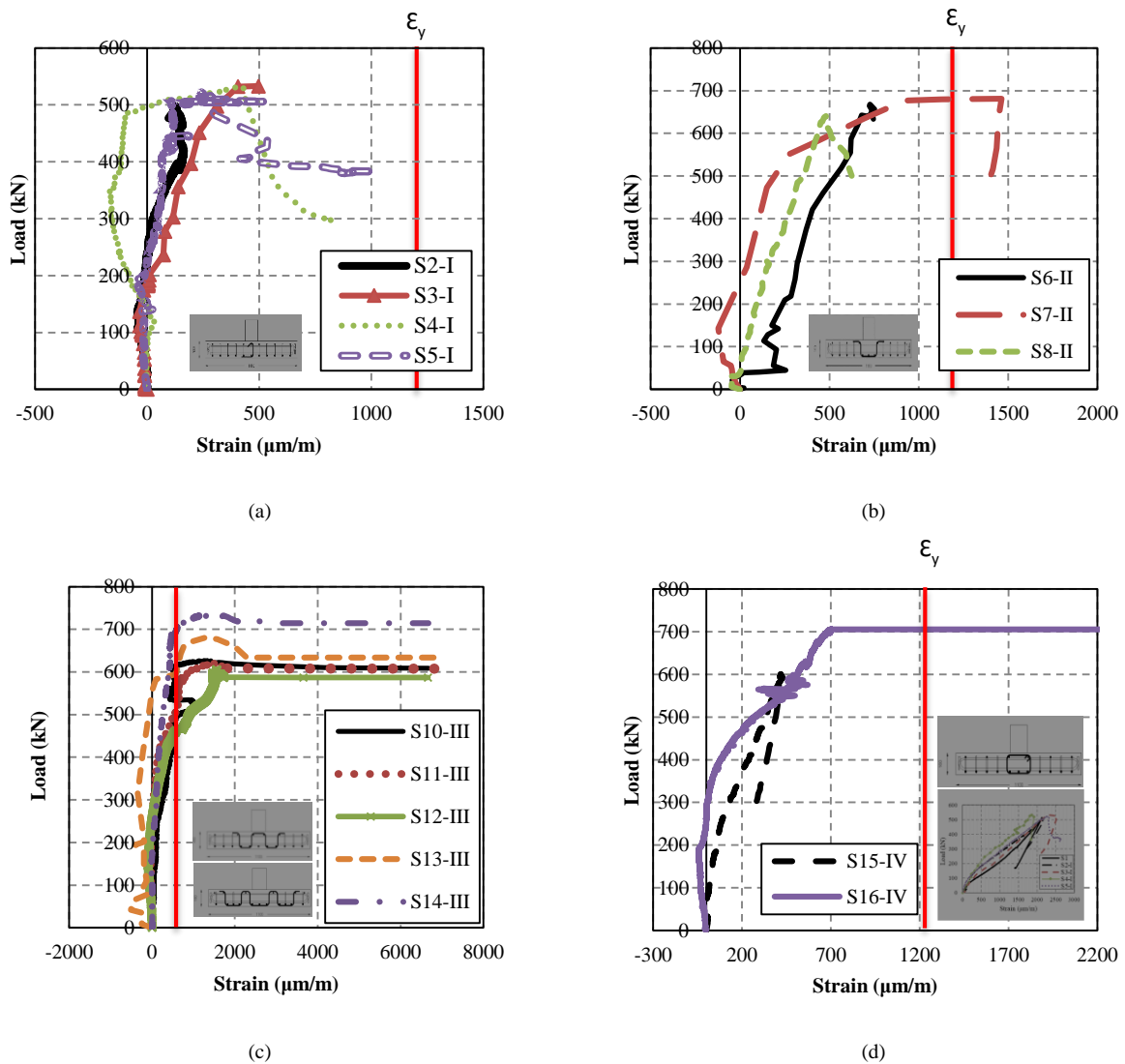
Figure 24. Load strain curve for stirrup at 50mm from column of: (a) Group I, (b) Group II, (c) Group III, and (d) Group IV

4. Finite Element Investigation

In this section, a numerical investigation using three-dimensional finite element analysis is conducted on the tested specimens to further evaluate the punching behavior of the column-slab connections using shear reinforcement and with the aim of reaching a suitable design approach for estimating the punching capacity of the slabs. The commercial program ANSYS version 19 R1 [21] was used in this study.

4.1. Finite Element Model

Three-dimensional finite element models (FEM) were generated for one quarter of the slab using the finite element analysis program ANSYS version 19 R1 [21] for all sixteen tested slabs. The ANSYS element library contains more than 100 different element types. Each element type used has a unique number and a prefix that identifies the element category. To model concrete parts, the Solid 65 element was used as shown in Figure 25-a. The solid 65 element has 8 nodes with three degrees of freedom at every one of them. This element can show cracking in tension, crushing in compression, and plastic deformation. For the steel reinforcement, Link 180 was used which is an axial rod element having 2 nodes each with three degrees of freedom as shown in Figure 25-b. The element can show plastic deformation typical for steel reinforcement. Link 180 elements were modeled using the discrete method and the nodes were connected to those of the solid concrete elements assuming perfect bond between steel and concrete.
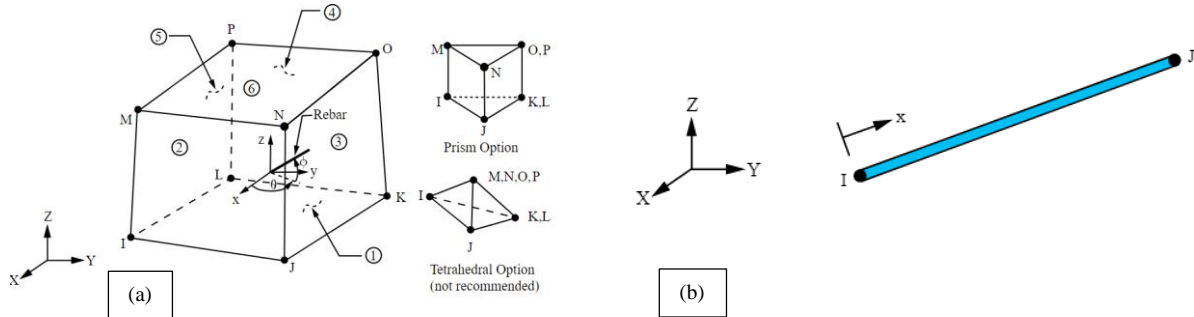
Figure 25. Structural elements used in the finite element analysis a) SOLID65 (b) LINK180 [21]

The quarter of each slab was modeled using a 3D mesh with fine elements having a maximum regular size of 25 mm. Figure 26 shows elements, meshing, and boundary conditions for the typical quarter model used in the analysis. Figure 27 shows the typical boundary conditions for the finite element models which was chosen to simulate the actual conditions applied during the experimental testing.
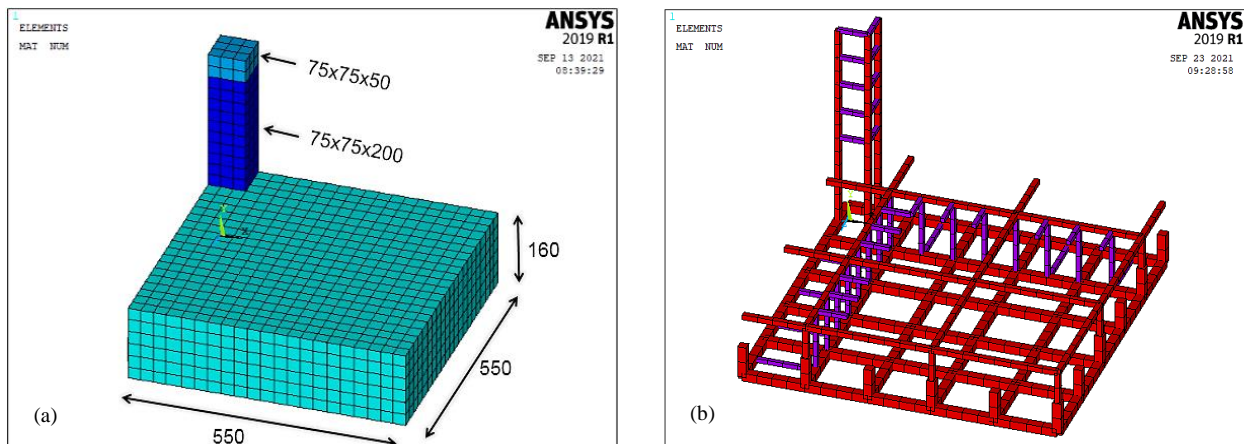
Figure 26. FEM modeling a) Solid 65 dimensions and meshing b) Link 180 meshing for Group II (Typical)
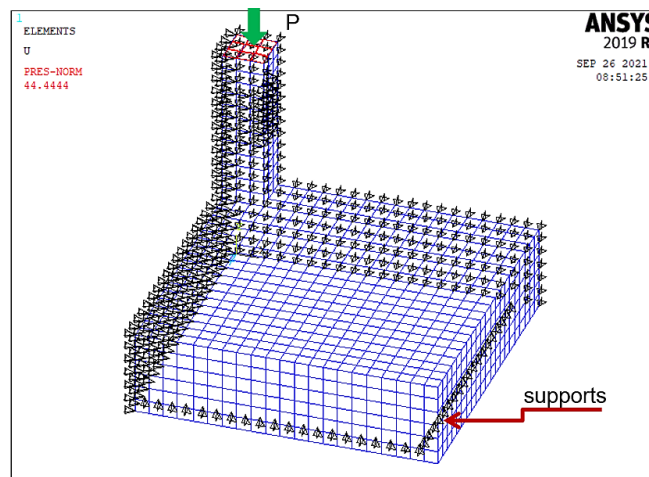
Figure 27. The boundary conditions used in the FEM modeling

4.2. Material Modeling and Parameters

The stress-strain relationship used for concrete in compression is shown in Figure 28 (a) while the idealized stress-strain curve for the main reinforcing steel bars and stirrups are shown in Figure 27(b) and (c) respectively. The actual value of the characteristic compressive strength of concrete obtained from cube testing was used in the modeling. While the concrete tensile strength was assumed to be $0.6\sqrt{f_c'}$ (MPa) as per ACI 318-19 [2]. Poisons ratio used for concrete was assumed to be 0.2 while 0.3 was used for steel. The modulus of elasticity used for concrete was assumed to be $4700\sqrt{f_c'}$ (MPa) as per ACI 318-19 [2] while 200 GPa was used for the reinforcing steel. The shear retention crack, β, used was 0.2 for open cracks and 0.8 for closed ones.

(a)

(b)

(c)
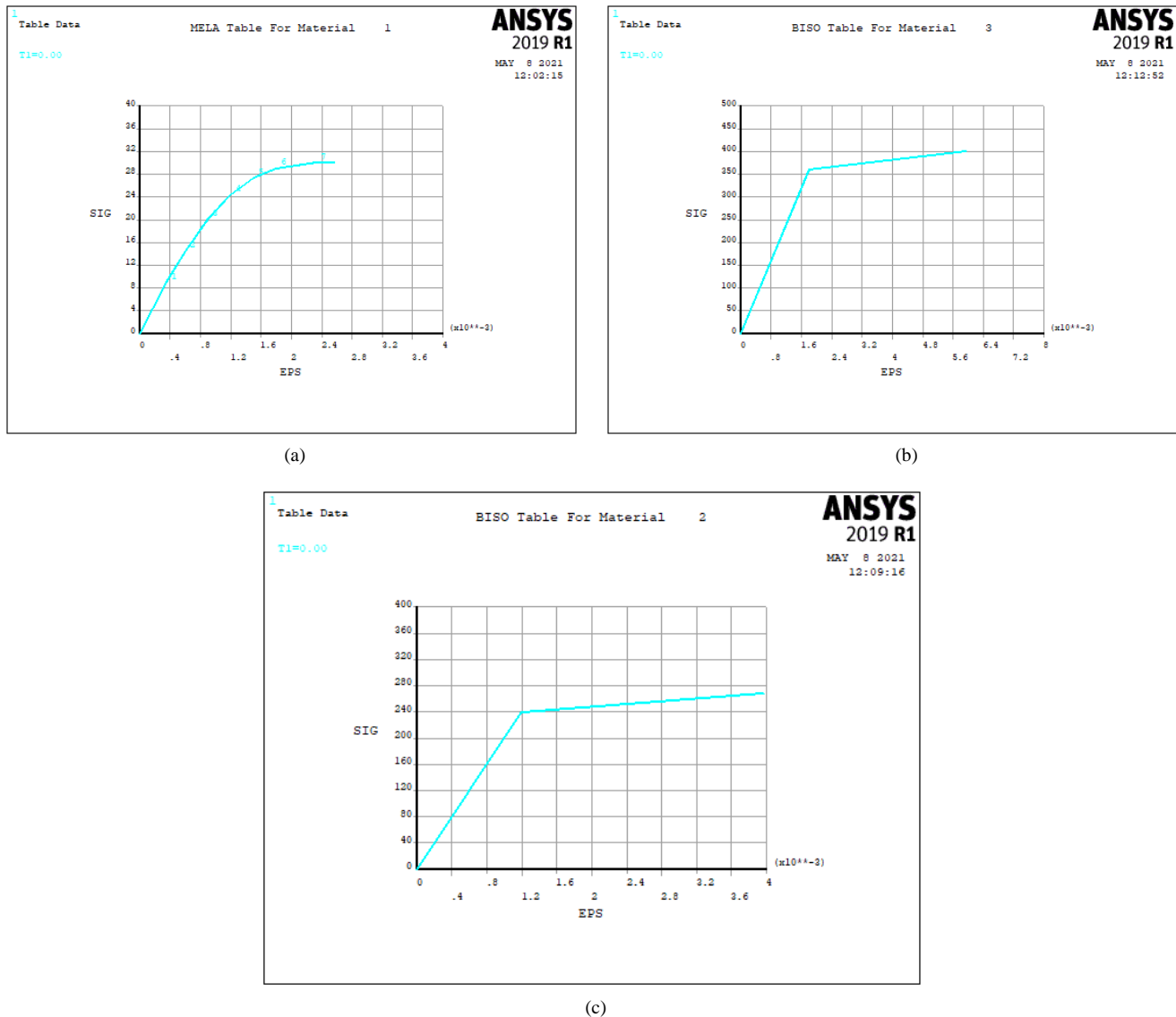
Figure 28. Typical Stress-Strain Curve for: (a) concrete (b) deformed steel bars (c) mild steel bars

4.3. Finite Element Analysis and Results

A quasi-Newton–Raphson method was used for the iteration process where the unbalanced load vector representing the difference between the material strength and the applied load is calculated step by step [21].

Results of the finite element analysis are listed in Table 3. In general, the average ratio of the finite element analysis results and the experimental results for all specimens is about 26%. It should be noted that the results obtained by the ANSYS program are 20% higher than the experimental results for the specimens reinforced with single-leg, multi-leg stirrups having 4-branches, and closed stirrups having 2-branches. The deviation between numerical and experimental results of some of the specimens can be due to the fact that the compressive and tensile stress-strain properties of concrete may differ between those used in the analytical model and the actual stress-strain behavior of the tested slabs. Since the percentage of error exceeded 20% for the ultimate load of some specimens, the finite element analysis needs more investigation which will be further studied in succeeding research and an extensive parametric study will be presented.

The aim of using the finite element analysis is to be able to analyze a larger number of parameters and conduct more in-depth investigation on the behavior of slabs with shear reinforcement that may not be possible to perform experimentally.

Table 3. Comparison between experimental and computed values of ultimate loads

| Specimen ID | Vu-test (kN) | V_{ANSYS} | Vu-code (kN) | | | | | | Vu-test/ Vu-code | | | | | | V_{ANSYS} / Vu- test |
| | | | ACI 318-19 | | | ECP 203-2018 | | | ACI 318-19 | | | ECP 203-2018 | | | |
			At d/2 from column	At d/2 from outer perimeter	Maximum set by the code	At d/2 from column	At d/2 from outer perimeter	Maximum set by the code	At d/2 from column	At d/2 from outer perimeter	Maximum set by the code	At d/2 from column	At d/2 from outer perimeter	Maximum set by the code	
S1 (control)	515	581.3	229.3		347.5	245.5		349.7	2.2		1.5	2.1		1.5	1.13
S2-I	498	671.88	243.7	267	367.9	224.3	539	370.2	2.0	1.87	1.4	2.2	0.92	1.3	1.35
S3-I	533	690.38	359.6	261	359.6	347.6	539	361.8	1.5	2.04	1.5	1.5	0.99	1.5	1.30
S4-I	532.5	693.41	247.8		359.6	222		361.8	2.1		1.5	2.4		1.5	1.30
S5-I	524	697.17	373.6		359.6	347.6		361.8	1.4		1.5	1.5		1.4	1.33
S6-II	668	762.31	387.4	325.4	400.8	358.6	602.8	403.3	1.7	2.05	1.7	1.9	1.11	1.7	1.14
S7-II	681.5	840.32	638.47	325.4	400.8	609.7	602.8	403.3	1.1	2.09	1.7	1.1	1.13	1.7	1.23
S8-II	640.5	770.86	376.18		367.9	349.8		370.2	1.7		1.7	1.8		1.7	1.20
S9-II	688	825.74	627.3		367.9	600.9		370.2	1.1		1.9	1.1		1.9	1.20
S10-III	627	823.87	387.4	356.1	400.8	358.6	659.8	403.3	1.6	1.76	1.6	1.7	0.95	1.6	1.31
S11-III	620	860.13	640.2	356.1	405.9	611.1	659.8	408.4	1.0	1.74	1.5	1.0	0.94	1.5	1.39
S12-III	606.5	841.12	389.1		405.9	360		408.4	1.6		1.5	1.7		1.5	1.39
S13-III	682.5	929.11	640.2		405.9	611.1		408.4	1.1		1.7	1.1		1.7	1.36
S14-III	736	826.91	620.3		347.5	595.4		349.7	1.2		2.1	1.2		2.1	1.12
S15-IV	600	775.75	387.4		400.8	358.6		403.3	1.5		1.5	1.7		1.5	1.29
S16-IV	706.5	814.78	347.5		369.25	344.3		349.7	2.0		2.0	2.1		2.0	1.15
Average									1.6	1.93	1.6	1.6	1.0	1.6	1.26

5. Comparison with Code Predictions

Generally, the punching shear stress evaluation in design codes is conducted at a critical section located at a distance from the face of the column support and the ultimate punching shear capacity of concrete is taken as a function of the concrete compressive strength. The shear reinforcement represents a component of the punching capacity if present and in some cases the flexural reinforcement ratio is considered. In this section, the provisions provided by ACI 318-19 [1] and ECP 203-2018 [2] are investigated and the test results are compared to those predicted by the two mentioned design codes. Two critical sections need to be considered. The inner critical section which is defined at d/2 from the face of the column and the outer critical section which is defined at d/2 from the last row of shear reinforcement as shown in Figure 29.

According to the ACI 318-19 [1] design shear strength is the least of the two values obtained by Equations 2 and 3 at the inner critical section and is the value obtained by Equation 4 at the outer critical section. All equations are in SI units.

$$v_u = 0.33\sqrt{f_c'} \tag{2}$$

$$v_u = 0.17\sqrt{f_c'} + \frac{A_v f_{yt}}{b_o s} \leq 0.5\sqrt{f_c'} \tag{3}$$

$$v_u = 0.17\sqrt{f_c'} \tag{4}$$

where f_c' is the cylinder concrete strength and is equal to about 80% of f_{cu}, s is spacing between stirrups, A_v is the cross-sectional area of all legs of reinforcement on one peripheral line that is geometrically similar to the perimeter of the column section within spacing s, f_{yt} is the yield stress of the shear reinforcement, and b_o is the critical shear perimeter at d/2 from the face of the column where d is the effective depth of the slab.
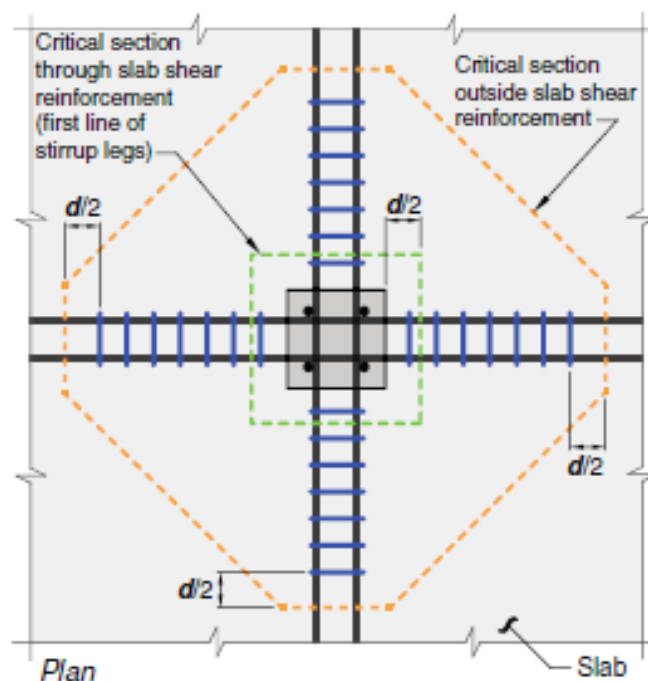
Figure 29. Location of critical sections for punching [1, 2]

According to the ECP 203-2018 [2] design strength values are limited by the minimum of the two Equations 5 and 6 at the inner critical section and is the value obtained by Equation 5 at the outer critical section. All equations are in SI units:

$$v_u = 0.316\sqrt{\frac{f_{cu}}{\gamma_c}} \tag{5}$$

$$v_u = 0.12\sqrt{\frac{f_{cu}}{\gamma_c}} + \frac{A_{st}f_y}{b_o s \gamma_s} \leq 0.45\sqrt{\frac{f_{cu}}{\gamma_c}} \tag{6}$$

where f_{cu} is characteristic cube concrete strength, γ_c and γ_s are reduction factor for concrete and steel strength respectively, s is spacing between stirrups, A_{st} is the cross-sectional area of all legs of reinforcement on one peripheral line that is geometrically similar to the perimeter of the column section within spacing s, and f_y is the yield stress of the shear reinforcement.

The comparison in Table 3 shows that the ratios Vu-test/Vu-code according to both design codes were generally conservative. For the control specimen, the ACI 318-19 [1], is slightly more conservative than the ECP 203-2018 [2]. The reason for the underestimated values predicted by both codes is that the ultimate capacity for concrete is the governing equation in predictions especially for specimens having stirrups at a spacing of 25 mm. Although ECP 203-2018 [2] and ACI 318-19 [1] codes have nearly the same result at the inner critical section, ECP 203-2018 [2] gives overestimated results at the outer perimeter. The reason for the overestimated values predicted by ECP 203-2018 [2] at the outer perimeter is due to using equation (5) with the uncracked strength of concrete instead of the cracked strength as per ACI 318-19 [1] (Equation 4). This means that this calculation could lead to unsafe designs according to ECP 203-2018 [2]. Finally, although all specimens had a thickness of 160 mm which is less than the values recommended by the ECP 203-2018 [2] and the ACI 318-19 [1], the use of stirrups in the vicinity of the slab column connection significantly increased the punching strength.

6. Conclusions

Based on the results of the experimental program conducted on 16 column-slab specimens, the analytical computation using ANSYS V19R1 and the evaluation using design codes, several conclusions are drawn as follows:

- All slabs failed in punching showing the three typical modes of failure where the failure surface occurred within the shear reinforcement zone or outside the shear reinforcement zone and only for specimen S15-IV crushing of the concrete strut near the column face was observed.

- The mode of failure was affected by the number of legs used in the stirrups. Specimens having four and six legs showed a mixed flexural-punching mode of failure.

- Using shear reinforcement in the form of single leg stirrups showed insignificant improvement in punching strength and ductility. This is due to the arrangement in the perpendicular form causing large spacing in the

tangential directions. It is recommended to study different arrangements in the radial direction to improve the slab behavior in this case.

- For the range of shear reinforcement ratios studied in this research, using multi-leg open or closed stirrups, the punching capacity increased by up to 40% compared to the specimen without shear reinforcement. The deformation was also significantly improved.

- At the same reinforcement ratio, the effect of increasing stirrups width on the shear capacity was insignificant. However, ductility was improved.

- Closed stirrups with four legs showed the highest improvements in terms of ductility. In this research, limited number of specimens with closed stirrups were used. More extensive experimental program is needed to estimate the punching strength in case of using closed stirrups with a wider range of parameters.

- Extending stirrups beyond the outer punching critical section specified by the design codes (at 2d from face of the support) has minor effects on the punching shear strength.

- Experimental readings of strain in stirrups indicated that yielding generally occurred in case of multi leg stirrups showing better performance of shear reinforcement in this case.

- The finite element computation using ANSYS overestimated the shear strength of all specimens with stirrups. Further investigations are still needed for enhancement of the output results.

- The expressions in both the ACI 318-19 and the ECP 203-2018 for predicting the punching strength at the critical section located at d/2 from column face yielded values that were conservative compared to the test results. While the expression in ECP 203-2018 for predicting punching strength at the critical section located at d/2 beyond the outermost peripheral line of shear reinforcement could lead to unsafe design.

- The test results in this research showed punching strength improvement when using shear reinforcement in slabs with thickness less than the limit set by the design codes. It is recommended to expand the experimental program to estimate the adjustments needed so that lower slab thickness reinforced with multi-leg or closed stirrups can be used to design flat-plate column connections safely.

7. Declarations

7.1. Author Contributions

The main ideas and the methodology of the research were discussed and decided by all the authors. The FEM using software was conducted by G.Y. The manuscript was written by M.M. and G.Y. and the review was done by O.R. The results, discussions, interpretation, and conclusion were completed by all authors. All authors have read and agreed to the published version of the manuscript.

7.2. Data Availability Statement

The data presented in this study are available in the article.

7.3. Funding

The authors received no financial support for the research, authorship, and/or publication of this article.

7.4. Conflicts of Interest

The authors declare no conflict of interest.

8. References

[1] Lips, S., Fernández Ruiz, M., & Muttoni, A. (2012). Experimental investigation on punching strength and deformation capacity of shear-reinforced slabs. ACI Structural Journal, 109(6), 889-900. doi:10.14359/51684132.

[2] ACI Committee 318-19. (2019). Building Code Requirements for Structural Concrete. American Concrete Institute (ACI), Farmington Hills, United States. doi:10.14359/51716937.

[3] ECP 203-2018. (2018). Egyptian Building Code for Structural Concrete Design and Construction. Ministry of Housing, Utilities & Urban Communities, Cairo, Egypt.

[4] EN 1992-1-1. (2004). Eurocode 2: Design of concrete structure-Part 1-1: General rules and rules for buildings. European Committee for Standardization, Brussels, Belgium.

[5] Papanikolaou, K. V., Tegos, I. A., & Kappos, A. J. (2005). Punching shear testing of reinforced concrete slabs, and design implications. Magazine of Concrete Research, 57(3), 167–177. doi:10.1680/macr.2005.57.3.167.

[6]   Hegger, J., Sherif, A. G., Kueres, D., & Siburg, C. (2017). Efficiency of Various Punching Shear Reinforcement Systems for Flat Slabs. ACI Structural Journal, 114(3), 631–642. doi:10.14359/51689434.

[7]   Mabrouk, R. T. S., Bakr, A., & Abdalla, H. (2017). Effect of flexural and shear reinforcement on the punching behavior of reinforced concrete flat slabs. Alexandria Engineering Journal, 56(4), 591–599. doi:10.1016/j.aej.2017.05.019.

[8]   Broms, C. E. (2019). Cages of inclined stirrups as shear reinforcement for ductility of flat slabs. ACI Structural Journal, 116(1), 83–92. doi:10.14359/51710871.

[9]   Issa, A. M., Salem, M. M., Mostafa, M. T., Hadhoud, H. M., & Ghit, H. H. (2019). Performance of Shear Reinforcement against Punching Shear Loads. International Journal of Engineering and Advanced Technology, 9(2), 841–850. doi:10.35940/ijeat.b3975.129219.

[10] Schmidt, P., Kueres, D., & Hegger, J. (2020). Punching shear behavior of reinforced concrete flat slabs with a varying amount of shear reinforcement. Structural Concrete, 21(1), 235–246. doi:10.1002/suco.201900017.

[11] Raafat, A., Fawzi, A., Metawei, H., & Abdalla, H. (2021). Assessment of stirrups in resisting punching shear in reinforced concrete flat slab. HBRC Journal, 17(1), 61–76. doi:10.1080/16874048.2021.1881422.

[12] Polak, M. A., El-Salakawy, E., & Hammill, N. L. (2005). Shear reinforcement for concrete flat slabs. Special Publication, 232, 75-96.

[13] Broms, C. E. (1990). Shear reinforcement for deflection ductility of flat plates. ACI Structural Journal, 87(6), 696–705. doi:10.14359/2988.

[14] Broms, C. E. (2000). Elimination of flat plate punching failure mode. ACI Structural Journal, 97(1), 94–101. doi:10.14359/838.

[15] Eom, T. S., Kang, S. M., Choi, T. W., & Park, H. G. (2018). Punching shear tests of slabs with high-strength continuous hoop reinforcement. ACI Structural Journal, 115(5), 1295–1305. doi:10.14359/51702231.

[16] Beutel, R., & Hegger, J. (2002). The effect of anchorage on the effectiveness of the shear reinforcement in the punching zone. Cement and Concrete Composites, 24(6), 539–549. doi:10.1016/S0958-9465(01)00070-1.

[17] Yang, Y., Li, Y., Guan, H., Diao, M., & Lu, X. (2021). Enhancing post-punching performance of flat plate-column joints by different reinforcement configurations. Journal of Building Engineering, 43, 1–17. doi:10.1016/j.jobe.2021.102855.

[18] Hugo Dalosto de Oliveira, V., Jorge Nery de Lima, H., & Sales Melo, G. (2022). Punching shear resistance of flat slabs with different types of stirrup anchorages such as shear reinforcement. Engineering Structures, 253, 113671. doi:10.1016/j.engstruct.2021.113671.

[19] Ghali, A., Neville, A. M., & Brown, T. G. (2017). Structural Analysis: A unified classical and matrix approach (6th Ed.). CRC Press, Boca Raton, United States. doi:10.1201/9781315273006.

[20] Einpaul, J., Brantschen, F., Ruiz, M. F., & Muttoni, A. (2016). Performance of Punching Shear Reinforcement under Gravity Loading: Influence of Type and Detailing. ACI Structural Journal, 113(4). doi:10.14359/51688630.

[21] ANSYS Mechanical APDL Manual Set. (2019). ANSYS Software Company, Pennsylvania, United States.